



# Effect of alkaline treatment on the thermo-physicochemical and mechanical properties of biochar powder/*Washingtonia robusta* fibers/PLA hybrid biocomposites

Isma Dembri<sup>a</sup>, Ahmed Belaadi<sup>a,\*\*</sup>, Abdelaziz Lekrine<sup>a</sup>, Mohammad Jawaid<sup>b,\*</sup>, Ahmad Safwan Ismail<sup>c</sup>, Djamel Ghernaout<sup>d,e</sup>

<sup>a</sup> Department of Mechanical Engineering, Faculty of Technology, University 20 August 1955, Skikda, El-Hadaiek, Skikda, Algeria

<sup>b</sup> Chemical and Petroleum Engineering Department, College of Engineering, United Arab Emirates University (UAEU), PO Box, 15551, Al Ain, United Arab Emirates

<sup>c</sup> Department of Bio-composite Laboratory, Institute of Tropical Forestry and Forest Products, Universiti Putra Malaysia, 43400, UPM Serdang, Selangor, Malaysia

<sup>d</sup> Chemical Engineering Department, College of Engineering, University of Ha'il, PO Box 2440, Ha'il, 81441, Saudi Arabia

<sup>e</sup> Chemical Engineering Department, Faculty of Engineering, University of Blida, PO Box 270, Blida, 09000, Algeria

## ARTICLE INFO

Handling editor: SN Monteiro

### Keywords:

*Washingtonia robusta*

Biocomposite

Bioplastic/PLA matrix

thermal properties

Mechanical properties

## ABSTRACT

Replacing plastic products with fully biodegradable products remains a challenge in our daily lives. Biodegradable hybrid bio composites are designed for various structural and non-structural applications such as car interiors, filaments for 3D printers, biomedical, sports and electronic products, green building materials and food packaging. In this work hybrid composites fabricated using polylactic acid (PLA) matrix reinforced with short plant fibers from the *Washingtonia robusta* (WR) palm tree and biochar powder (BC) with grain diameters less than 0.6 μm obtained from WR palm waste after carbonization at 300 °C. Initially, a portion of the untreated plant fibers was retained, while the other portion was treated with NaOH (1, 2, 3%) for 15 h. Indeed, the untreated and alkali-treated fibers were observed by SEM and then characterized by thermogravimetric analysis/differential scanning calorimetry. Fourier transform infrared showed physical and chemical changes with surface degradation of the WR treated at higher concentrations (3% NaOH). In addition, establish the relationship between the alkali treatments of the biocomposite reinforcement fibers and the improvement of the mechanical performance of these materials. The best results obtained for the developed biocomposite hybrid products are those of BTR3, for mechanical characteristics such as traction, flexural strength and Izod, with values of 39.56 MPa and 74.43 MPa, and 3.26 kJ/m<sup>2</sup> respectively; and 2.30 MPa as elastic stress, also for water absorption with a percentage of 8.3%. The percentages of the alkaline treatments used revealed that the BTR3 model presents the best physical-chemical and mechanical behavior of these new materials.

## 1. Introduction

The introduction of biocomposite materials founded on using biodegradable matrices and natural reinforcements into industry continues to grow [1]. The gradual decline in underground energy resources [2] and the problem of eliminating plastic from the environment worry researchers about replacing these non-degradable composites despite the increasing use of the planet's wealth in industrial production worldwide [3,4] In addition to their low density, which gives them good mechanical properties compared with synthetic fibers [5,6], statistics over the last decade have shown that only 6% of thermoplastic materials

are recycled [7,8]. Biocomposites with polylactic acid (PLA) matrix reinforced with natural fibers have been around since the 1970s [9].

Their improvement is an ongoing process, with the adoption of new techniques like plant fibers' chemical treatments in reinforcing, adding different fibers (hybrid fibers) to offer superior mechanical properties to thermoplastic composites and thus replace glass and metals, reducing the greenhouse effect that threatens life on the planet [10,11]. Biocomposites offer more advantages than synthetic ones: they are lighter and resist impact and fatigue well, withstand humidity and heat well, are nature's friend, and do not give off toxic gases when incinerated, and their natural tendency makes them non-corrosive. These degradable materials are destined for various economic and industrial markets. In

\* Corresponding author.

\*\* Corresponding author.

E-mail addresses: [a.belaadi@univ-skikda.dz](mailto:a.belaadi@univ-skikda.dz) (A. Belaadi), [jawaid@uaeu.ac.ae](mailto:jawaid@uaeu.ac.ae) (M. Jawaid).

<https://doi.org/10.1016/j.jmrt.2024.12.018>

Received 28 August 2024; Received in revised form 22 November 2024; Accepted 1 December 2024

Available online 3 December 2024

2238-7854/© 2024 The Authors. Published by Elsevier B.V. This is an open access article under the CC BY license (<http://creativecommons.org/licenses/by/4.0/>).

### Abbreviations

ANNs	Artificial neural networks
BCH	Biochar
CI	Crystallinity index
CS	Crystal size
DSC	Differential scanning calorimetry
DTG	Derivative thermogravimetry
FTIR	Fourier transform infrared
GL	Gauge length
ML	Maximum likelihood
SEM	Scanning electron microscope
SR	<i>Syagrus romanzoffiana</i>
TGA	Thermogravimetric analysis
WF	<i>Washingtonia filifera</i>
WR	<i>Washingtonia robusta</i>
WRF	<i>Washingtonia robusta</i> fiber
PLA	Polylactic acid
TS	Tensile strain ( $\epsilon$ )
YTF	<i>Yucca treculeana</i> fiber

the food packaging industry, they are found in large quantities in disposable cups and plates, bottles and tins, films, and food bags. They can be used for new generations of prostheses as tissue-based sensor [12], or highly elastic strain sensors [13], orthopedic implant pins, and pharmaceutical products such as dental or suture threads, tablet blister packs, or even spectacle frames. Another broad field in consumer markets is cosmetics, hygiene, and cleanliness products, such as sanitary products (nappies, wipes, handkerchiefs, etc.) and various makeup product packaging. The composite materials can be used in 3D printing for different applications, such as those in the robotics and electronics field [14] as well in flexible piezoresistive sensor [15], they can also be used in producing parts and coatings in the space industry, aeronautics (aircraft wings [16]), as well as in automotive interior parts, not forgetting biocomposite materials' widespread incorporation in the building industry [17] or in the form of geopolymers. In this regard, Workiye and Woldsenbet [18] introduced corn stalk fibers as reinforcement for a kaolinite clay-based geopolymer using a retting process. These fibers were treated with 98% NaOH alkaline solution for 30 min. Their mechanical results indicated a strength of 1.184 MPa and a Young's modulus of 16 GPa. Additionally, incorporating 1.5 wt% of corn cellulose stem fibers into the geopolymer matrix increased the flexural strength to a range of 13.298–31.8 MPa, which is 2.4 times higher than that in Ref. [19].

Most biocomposites are highly crystalline materials that contain solid, rigid plant fibers with a low density, making them more flexible and recyclable, with less negative impact on the air, flora, and fauna. Many researchers are studying the total biodegradability of biocomposites and nature conservation, which has led them to focus on more and more different types of cellulose fibers to develop new materials. As such, Belaadi et al. [20] who studied mechanical properties and thermal, and physicochemical physical and morphological characterization of *Yucca treculeana* fibers (YTFs). Ferfari et al. [21] collected a new plant fiber from the central part of the palm leaves of *Syagrus romanzoffiana* (SR) to reinforce biocomposite materials. Their thermo-physicochemical and mechanical analyses revealed temperature resistance of up to 352 °C with a cellulose crystallinity index (CI) of 40.81% and a crystal size (CS) of 11.4 nm. The average  $\sigma_t$  was 671 MPa, the tensile strain ( $\epsilon$ ) was 1.84% at the break, and the elasticity  $E$  was 415 GPa. Research by Lalaymia et al. [22] focused on floral stem fibers extracted from the plant *Agave americana* L. These fibers contained crystallites with a CS of 2.53 nm and CI of 29.15%. While their average  $\sigma$  was  $64.34 \pm 11.43$  MPa, their  $E$  and  $\epsilon$  values were  $77.61 \pm 15.90$  GPa

and  $1.5 \pm 0.31\%$ , respectively.

Dembri et al. [23] examined the variation in unique mechanical characteristics like stress, strain, and Young's modulus on different batches of *Washingtonia filifera* (WF) fibers (WFFs) in the untreated, natural state to deduce the best number of fibers that gave the best mechanical performance of these fibers. They found that the batch of 120 untreated WFFs was the best. In another work researchers focused on the determination of the quasi-mechanical tensile parameters of fibers by varying the gauge lengths (GLs), such as Belaadi et al. [24], who examined several GLs (10, 20, 30, and 40 mm). Tensile tests were made on 120 fibers divided into four series to determine their diversity effects on the YTFs' mechanical properties ( $\sigma$ ,  $\epsilon$ , and  $E$ ). Boumaaza et al. [25] carried out a comparative study to predict the bending particularities of a bio-mortar in which they used the artificial neural networks (ANNs) and response surface methodologies (RSMs) models to examine the feasibility of using residues from the combustion of charcoal from the WF trunk biochar.

Researchers combined a biodegradable PLA matrix, which has a non-ordered crystalline structure, making it low-tenacity, plant fibers from the WF palm tree [23], and biochar from the same tree for complete elimination after use either by incineration [26] or ecological landfill treatment. PLA is a fully degradable plant resource obtained from sugarcane or corn starch. Reinforcement based on cellulose fibers has been used for various composites, degradable or polymeric [27,28]. Several investigators worked on the diversity of plant fibers applied as reinforcement in PLA-based biocomposites. Zhang et al. [29] studied the mixture of natural reinforcement containing bamboo fiber and coconut fiber as well as WF treated with PLA, then compared the results of the thermo-mechanical properties of the new combined composite with those of the coconut/PLA biocomposite. They also provided a new approach to introducing PLA-based biocomposites into industry, as the results have demonstrated significantly improved mechanical and thermal characteristics of the composite with three different types of reinforcement, plus an increase in durability, which directly impacts the biocomposite's lifespan.

In another work, investigators [30] studied PLA/cellulose composites for vegetable oil derivatives such as soybean oil, *Cleidiocarpum cavalier* oil, and flax oil as potential PLA plasticizers. Wang et al. [31] developed a biodegradable material of PLA matrix and aquatic bamboo by-product reinforcement modified with silane to increase the stability of the interactive relations between the cellulose and PLA where the water contact parameter of composite material has grown from 11.42° to 132.12°, with an improvement in its durability and a remarkable drop in the absorption rate (from 182.52% to 55.71%), which improved the water resistance characteristics of the material. In another interesting work, researchers' studies have confirmed that the quantity of fiber used improves the biocomposite's mechanical performance. Research by Ozyhar et al. [32] showed the influence of the number of reinforcing fibers in the PLA matrix. Different quantities of additional minerals ranged from 10%, 20%, 30%–40%. The results showed that 40% of the fiber reinforcement and 20% of the PLA weight improved the adhesion of the fibers between the filler and the matrix. Treatment with calcium carbonate preserved the biocomposite's mechanical characteristics while reducing the composite's PLA content.

Freitas et al. [33] studied the resistance and decomposition capacity of PLA single-layers, films, and fibers extracted from rice straw. The length of the reinforcement fibers is an important parameter. Sharma et al. [34] used two lengths of jute fiber, 140 and 9 mm, for a PLA matrix and obtained the best adhesion results with 140 mm long fibers. The reinforcement's chemical treatment is another critical factor directly influencing the fibers' adherence bonds at the interface. Khelifi et al. [35] studied the effect of alkaline treatment of WF palm lattice waste on improving the physical-mechanical features of the bio-mortar using test samples with ANN and RSM prediction methods. They treated these fibers with NaOH concentrations of 1–5% for 4–24 h. In another work analyzed on surface treatments of palm fibers with NaOH and NaHCO<sub>3</sub>

at a fixed concentration of 4% for different durations of 3, 7, 24, and 48 h [36]. This study was carried out by Koadri et al. [36] to develop and characterize improved interface adhesion with growth in the bending and compressive strength of the biocomposite. Another recent study by Dembri et al. [37] revealed that composites reinforced with non-NaOH-treated fibers could not withstand higher failure stresses than composites reinforced with alkali-treated fibers. This study examined biocomposite Epoxy's performance and delamination factor optimization based on NaOH-treated and non-NaOH-treated WFFs. Islam [38] studied the influence of chemical treatment with NaOH and Na<sub>2</sub>SO<sub>3</sub> on hemp fibers and epoxy and PLA matrices.

Various studies in the literature explore PLA/biomass biocomposites. The biochar/biomass functions as a liaison point in creating filament biocomposites in the parts' three-dimensional (3D) printing process [39]. It can also be a germination agent, facilitating the crystallization of the PLA matrix [40]. Incorporated with the PLA, it reinforces the matrix characteristics [41], promotes PLA crystallization [40], and perfects the biocomposites' thermal and mechanical characteristics [42]. In another study of Lekrine et al. [43], on hybrid biocomposites based on PLA matrix and coal waste filler from the same plant and reinforcement of WFFs treated with 10% NaHCO<sub>3</sub> for different treatment times, 72 h gave the best mechanical properties of these materials. The biochar will also facilitate demolding when designing the complex structures of these hybrid biocomposite materials, thereby helping to reduce costs. The reinforcement consists of raw cellulose fibers treated with three different concentrations of NaOH solution (1, 2, and 3%) for an immersion time of 15 h in NaOH.

Several researchers have studied the biodegradation properties of PLA as a biopolymer. Oka [44] examined the behavior of PLA/microcrystalline cellulose biocomposites and deduced that improving interfacial interactions of composites is associated with the optimization of the mechanical, dynamic, and static performance of composites, depending on the surface area of plant fibers. Brunsek et al. [45] showed the biodegradation of hemp, jute, and viscose plant fibers, all of which they buried under the ground for durations of 2, 4, 7, 9, and 11 days in specific environments. Then, they studied the effects of bacteria and fungi on the fiber's mechanical characteristics. These biocomposites will be intended for machining. To reduce material damage such as fractures and fiber detachment from the interface caused by grinding, Gao et al. [46] and Liu et al. [47] proposed several force models to minimize these damages and improve the mechanical performance of carbon fiber reinforced polymers [48].

In this context, this research aims to explore the thermal, physico-chemical, mechanical, and morphological properties of an innovative hybrid PLA biocomposite incorporating fibers extracted from WR palms. By applying various NaOH concentration treatments (1, 2 and 3%) over a period of 15 h, along with a load of 1% biochar sourced from the same palm tree, this study not only addresses existing gaps in the literature but also opens new approaches to renovation in the field of biocomposites and enhances the understanding of effective renovation strategies, thereby advancing practical applications in the development of environmentally friendly sustainable materials.

## 2. Experimental methods

The experimental methods used for the development and characterization of biocomposites can be divided into several essential steps, each requiring specific techniques to ensure a thorough and accurate analysis of the materials.

### 2.1. Materials

The WR palm, sometimes referred to as the Jupón palm, is abundant in the wild or cultivated for decoration, making its fibers less expensive. Its native country is Mexico, but it is also found on every continent, especially in South America, its continent of origin. It can also be found

in smaller quantities in Africa and Asia. The fibers used in this study are the raw fibers from the back of the Robusta palm obtained in Skikda, Algeria (Geographical coordinates are 36°45'33 "N 6°30'43 "E).

The vegetable reinforcement is a hybrid blend of 25% WR fiber (WRF) and 1% BCH powder. The fibers were extracted, decorticated, washed, and dried at an ambient temperature of 28 °C. The fibers were approximately 300 μm in diameter and cut to lengths of 2–5 mm, some of the fibers are recycled untreated while the second part was treated with NaOH by immersing it in the solution for 15 h at three concentrations (1, 2, and 3%). The BCH powder is derived from WR dead palm waste burnt at 300 °C, grinding, and then sieving to obtain grain diameters of less than 0.3–0.6 μm. The matrix used is PLA, which has a density of 1.26 g/cm<sup>3</sup> [49–52].

### 2.2. Fabrication of biocomposites

Several well-defined steps were carried out to develop the biocomposites. Before any operation, the matrix load and the mass of each component of the future material (Table 1) must be determined. Before mixing the elements in the mixer, the speed is set at 50 rpm at a temperature of 180 °C. The first stage begins with the PLA matrix, which is left to melt for 2 min, followed by adding the biomass filler and the WR reinforcement filler. After 10 min of mixing, the machine is stopped, and the biocomposite mixture is retired from the internal shafts and cut into short pieces. Next, the mixture is placed in a mold of dimensions (150 × 150 × 3 mm<sup>3</sup>). The mold is placed in a hydraulic press at T = 60 °C to form the sheets of material, then left to cool after demolding for 24 h in ambient air; in the end, the new green biocomposite is obtained (Fig. 1) and codified (Table 2).

### 2.3. Characterization method

The characterization methods for biocomposites are essential for evaluating their physical, mechanical, and chemical properties.

#### 2.3.1. Mechanical tensile testing of treated and untreated WR fibers

Tensile strength ( $\sigma$ ), strain ( $\epsilon$ ), and Young's modulus ( $E$ ) of untreated and treated fibers (with a series of 30 fibers) were analyzed under a 5 kN load of the Zwick Roell type at ambient temperature (23 °C), 40% humidity, and a test speed of 1 mm/min. The WRFs were tested with a GL of 40 mm and an average diameter measured with an optical microscope equal to 302 μm.

#### 2.3.2. Scanning electron microscope (SEM)

Surface analysis of WRFs (treated and untreated), BCH powder, and the biocomposites produced was conducted using the EM-30 AX plus (operational procedure of scanning electron microscope (SEM)) at different magnifications (10–100 μm). The samples were examined with an electron acceleration voltage of 20 kV.

#### 2.3.3. Fourier transform infrared (FTIR)

Fourier transform infrared (FTIR) spectroscopy is a working method based on measuring the infrared spectrum through the material's surface. The detection of vibrations characteristic of chemical bonds enables a topography of the chemical characteristics contained in the sample. The equipment used is the type region range 4000–525/ATR Method. Sixteen scans were collected, the average spectra were calculated from these twenty-four scans, and the baseline was corrected to

**Table 1**  
Load and mass of biocomposite components (PLA: polylactic acid).

Constituents	Load (%)	Mass (g)
Fibers	25	11.50
BCH	1	00.46
PLA	74	34.04

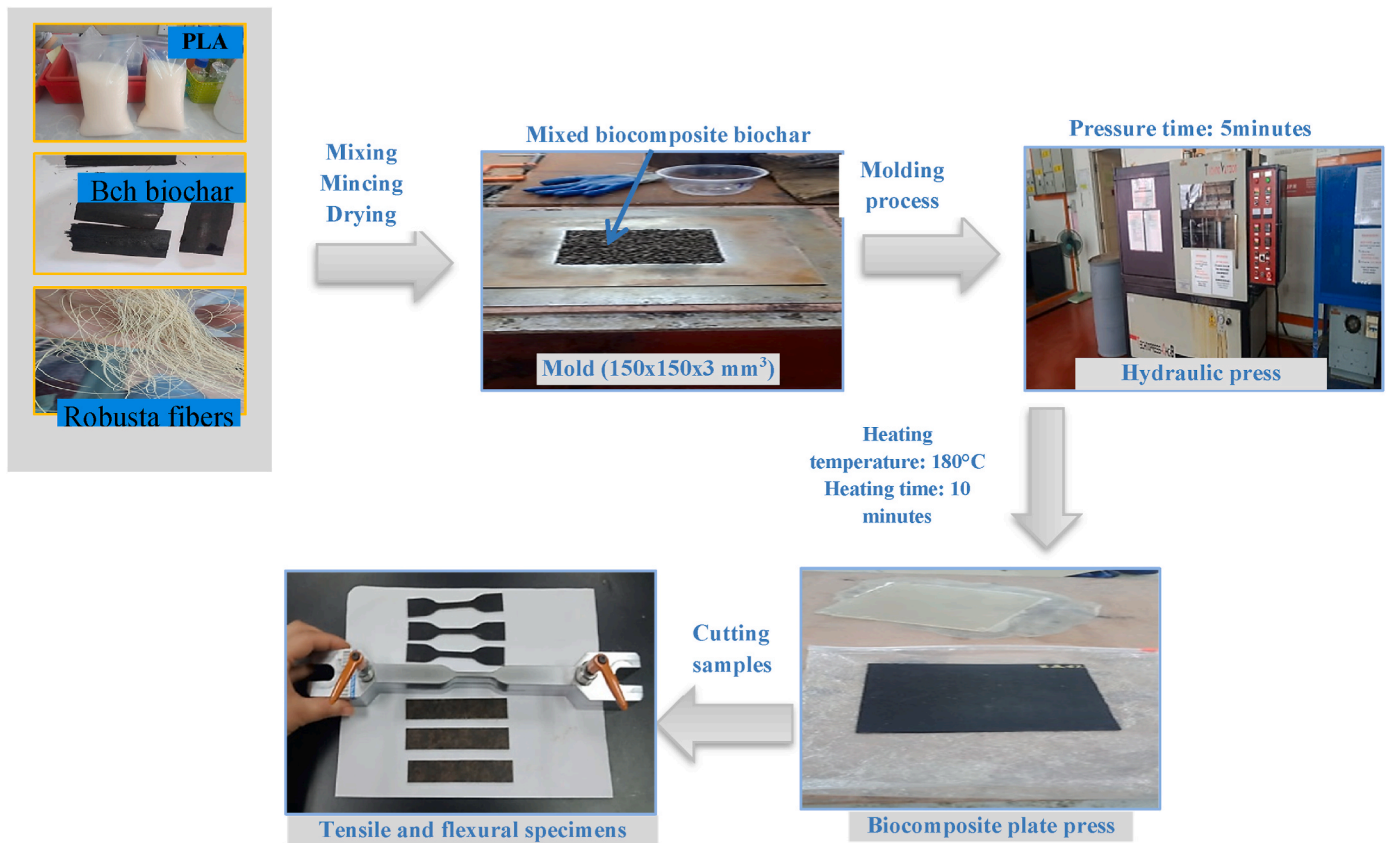


Fig. 1. Polylactic acid (PLA)/*Washingtonia robusta* (WR)-biochar (BCH) biocomposite development process and mechanical tests (tensile and flexure).

Table 2

Sample coding symbols for treated and untreated fibers and biocomposites (WR: *Washingtonia robusta*, WRF: *Washingtonia robusta* fiber, PLA: Polylactic acid, BCH: biochar).

Code	Fibers	Code	Biocomposite
UNWR	Untreated WRFs	UNB	PLA/UNWR-BCH1%
TR1WR	WRFs treated with 1% NaOH	BTR1	PLA/TR1WR-BCH1%
TR2WR	WRFs treated with 2% NaOH	BTR2	PLA/TR2WR-BCH1%
TR3WR	WRFs treated with 3% NaOH	BTR3	PLA/TR3WR-BCH1%

4000 cm<sup>-1</sup>.

### 2.3.4. Differential scanning calorimetry (DSC)

DSC analysis of all samples, either fibers (UNWR, T1WR, T2WR, T3WR) or biocomposites (PLA/UNWR-BCH 1%, PLA/T1WR-BCH 1%, PLA/T2WR-BCH 1%, and PLA/T3WR-BCH 1%; BCH: biochar), was carried out using a DSCQ20V24 machine. Using 11 Build 124 with a heating rate of 10 °C/min and a temperature of -50 to 300 °C before thermal decomposition, measurements were made in accordance with ASTM E2009-02 [53]. The test parameters were temperature (°C) and heat flux. The samples were 3 x 3 x 3 mm<sup>3</sup> and tested twice.

### 2.3.5. Thermogravimetric analysis (TGA)

TGA of the samples has been made on an instrument called TGAQ500V20.13 Build 39, under the ASTM E1131-03 standard, with sample dimensions of 3 x 3 x 3 mm<sup>3</sup>, a heating rate of 10 °C/min, and temperature up to 900 °C for the following test parameters: temperature (°C), weight (%), and weight derivative (%/°C).

### 2.3.6. Mechanical testing of PLA/WR-BCH biocomposites

A universal testing machine with a capacity of 30 kN at a constant

speed of 5 mm/min was used for tensile and flexural tests on samples molded according to ASTM D638 - 14 [54] with dimensions of 120 x 20 x 3 mm<sup>3</sup> and for bending tests according to ASTM D 790 -17 [55] with dimensions of 127 x 12 mm<sup>2</sup>. All tests were repeated three times at 24 °C and 50% humidity.

For the impact resistance tests on the plastic Izod pendulum, with impact energy conditions equal to 2.75 J and a test speed equal to 3.46 m/s, measurements of the impact parameters were made in accordance with ASTM D 256 [56]. The experiment was repeated for three samples measuring 63.5 x 12.7 x 3 mm<sup>3</sup>.

### 2.3.7. Water absorption test for all biocomposites produced

The influence of alkaline treatments at different concentrations (0, 1, 2 and 3%) of WRFs on water diffusion in the solid structure of the hybrid PLA/WR-BCH biocomposites produced. The specimens were cut to identical dimensions of 30 x 10 mm<sup>2</sup> and then subjected to dry polishing on three sides before being immersed in distilled water at an ambient temperature of 18 °C for 480 h. After each deep and complete immersion, we wiped the specimens with a smooth cotton wool cloth to avoid leaving drops of water on their surfaces, and finally weighed them on an electronic balance of 1/1000 (g) precision. The water absorption rate was calculated by ASTM D1037-99 [57]:

$$W (\%) = \left( \frac{m_h - m_s}{m_s} \right) \times 100 \tag{1}$$

where:  $m_h$ : mass of material after immersion (humid) and  $m_s$ : mass before immersion (dry).

### 3. Results and discussion

#### 3.1. Tensile properties analysis and Weibull statistics

To process the tensile mechanical property data for treated (3% NaOH concentration) and untreated WRFs, we chose the Weibull model

[58], which is well known for its use in treating brittle materials. The two-parameter Weibull distribution assumes that fiber failure is due to the degradation of the most brittle component [59,60] and is expressed by Eq. (2), where  $m$ ,  $s$ ,  $s_0$  are positive real numbers. The maximum likelihood (ML) method was used to determine and estimate the survival probability  $P$  (Eq. (3)), where  $\alpha = 0, 0.3, 0.375, \text{ and } 0.5$  and  $\Delta = 0, 0.25,$

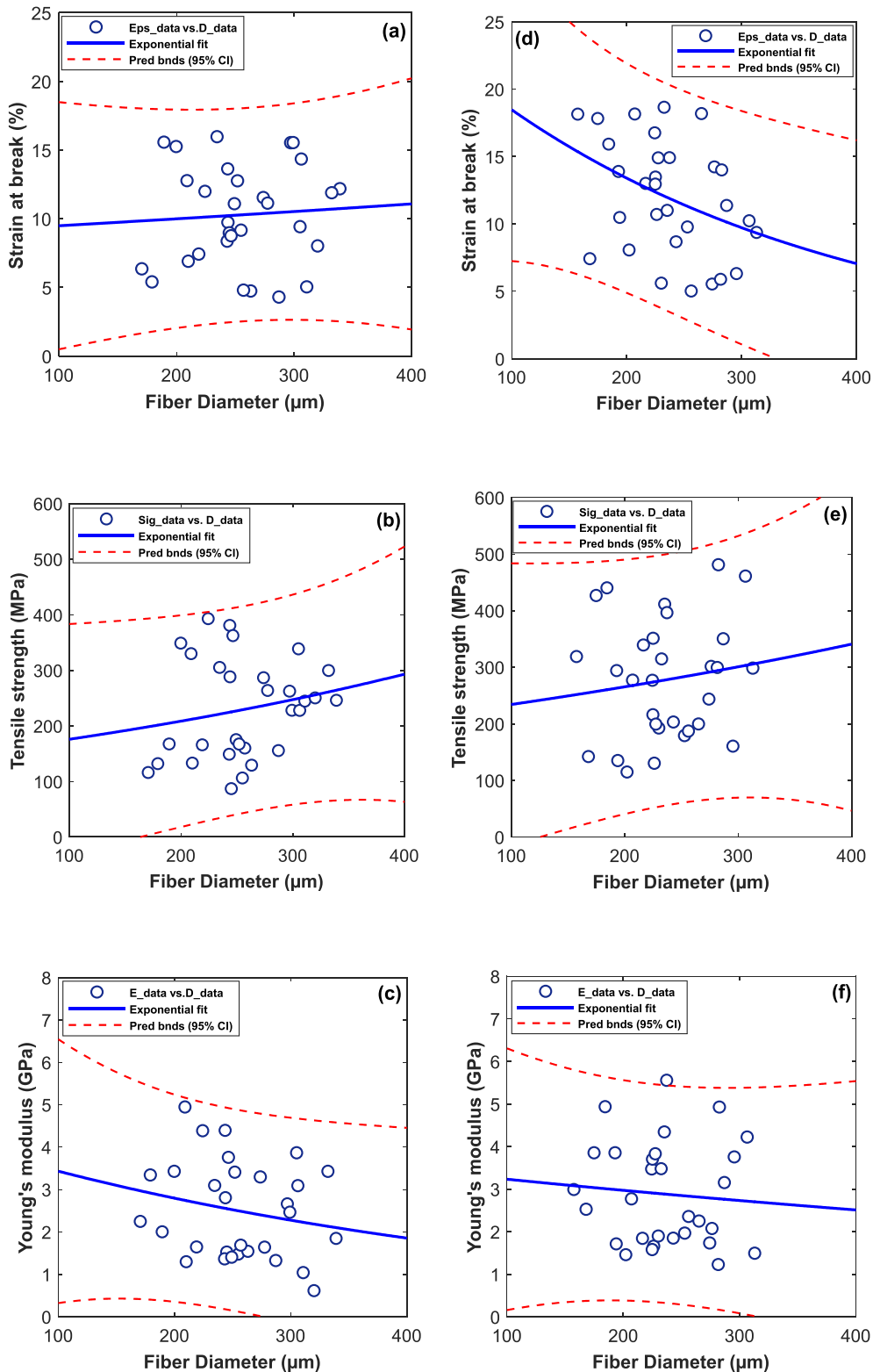


Fig. 2. Dispersion of mechanical properties as a function of fiber diameter (a-c) untreated and (d-f) treated fibers at 3% NaOH of WRfiber.

0.4, and 1. We used the Minitab software for this statistical method, which has a 95% confidence level (CL).

$$P(x|s, m) = 1 - e^{-\left(\frac{x}{s}\right)^m} \quad x \geq s_0 \quad (2)$$

$$P_i = \frac{i - \alpha}{n - \Delta} \quad (3)$$

Fig. 2 shows an exponential prediction model at 95% CL of the mechanical properties' dispersion as a function of diameter for the untreated fiber and that treated with 3% NaOH. The ratio between the fiber's diameter and the untreated fiber's ultimate strain differs for the two samples. In contrast, this strain grows with the increasing fiber diameter (Fig. 2a and d).

In addition, the tensile stress (at break) and Young's modulus follow the same evolution as a function of diameter for both fiber cases (Fig. 2b, c, e, and f), which indicates that when the stress increases, the elasticity modulus elasticity decreases, with minimal dispersion of the mechanical specifications in the treated fibers. These variations are due to the fibers' surface condition, structure, and geometry, which have become stiffer with alkaline treatment and have fewer impurities on their outer surface, not forgetting experimental conditions such as measurement errors, humidity, and temperature. This behavior is similar to that of WFFs reported by Dembri et al. [23].

These dispersions led us to conduct a prediction study of the mechanical behavior of WRFs treated at 3% and those untreated using the ML probability of the two-parameter Weibull distribution. Fig. 3 illustrates the experimental results for the 0% and 3% alkali-treated fibers, which follow a quasi-linear fit with a slight apparent offset between them. The results of this experiment show that strain at break, tensile stress, and modulus of elasticity for the treated fiber shift downwards with smaller values than those for the untreated fiber, which shift upwards with larger values. This behavior resembles others observed in the statistical analysis of the influence of alkaline treatment of date palm fruit branch fibers on their physico-mechanical behavior by Abderrezak et al. [61]. These results are directly related to the fibers' cellulosic structure. According to this ML statistical analysis, the lowest values were found in the population of fibers treated with 3% NaOH, in contrast to the untreated fiber, as in the date palm results of Amroune et al. [62], which makes the estimate very reliable.

The maximum results attained by the ML method of tensile stress at break, strain at break, Young's modulus (E) for 3% NaOH-treated fibers:  $\sigma_{TR3WR} = 243 \pm 45$  MPa,  $\epsilon_{TR3WR} = 12.07 \pm 41.28$  %, and  $E_{TR3WR} = 2.88 \pm 1.21$  GPa, are significantly higher than those of the untreated fibers:  $229 \pm 89$  MPa,  $10.28 \pm 3.66$ %, and  $2.51 \pm 1.4$  GPa, respectively, which are approaching those measured experimentally.

Table 3 indicates that the mechanical performances of TR3WR are more outstanding than those of fibers treated at 1 and 2% and that the tensile stress at break of TR3WR fibers is greater than that of WF according to Benzannache et al. [63] ( $119.3 \pm 86.28$  MPa), Lekrine et al. [64] ( $124.4 \pm 80.08$  MPa), and Dembri et al. [23] ( $204 \pm 111$  MPa). The same observation applies to the E. For this reason, more attention was focused on the physicochemical study of untreated and treated fibers and an analysis of the mechanical properties of biocomposites made from biodegradable PLA matrix, 1% palm biomass filler, and reinforcement of these WRFs untreated and treated with (1, 2 and 3%) NaOH concentration.

Fig. 4 describes the evolution of the probability of survival of the mechanical properties, according to Weibull's (ML) estimate, of the tensile strain ( $\epsilon$ ), tensile strength, and E of the raw fibers, and treated with 3% NaOH. The survival probability, which coincides nicely with the 50% of both samples, corresponds significantly to the Weibull (ML) estimates of the experimental results. The values of  $\sigma$ ,  $\epsilon$ , and E of the fiber treated with 3% NaOH are 243 MPa, 12.07 %, and 2.88 GPa, respectively.

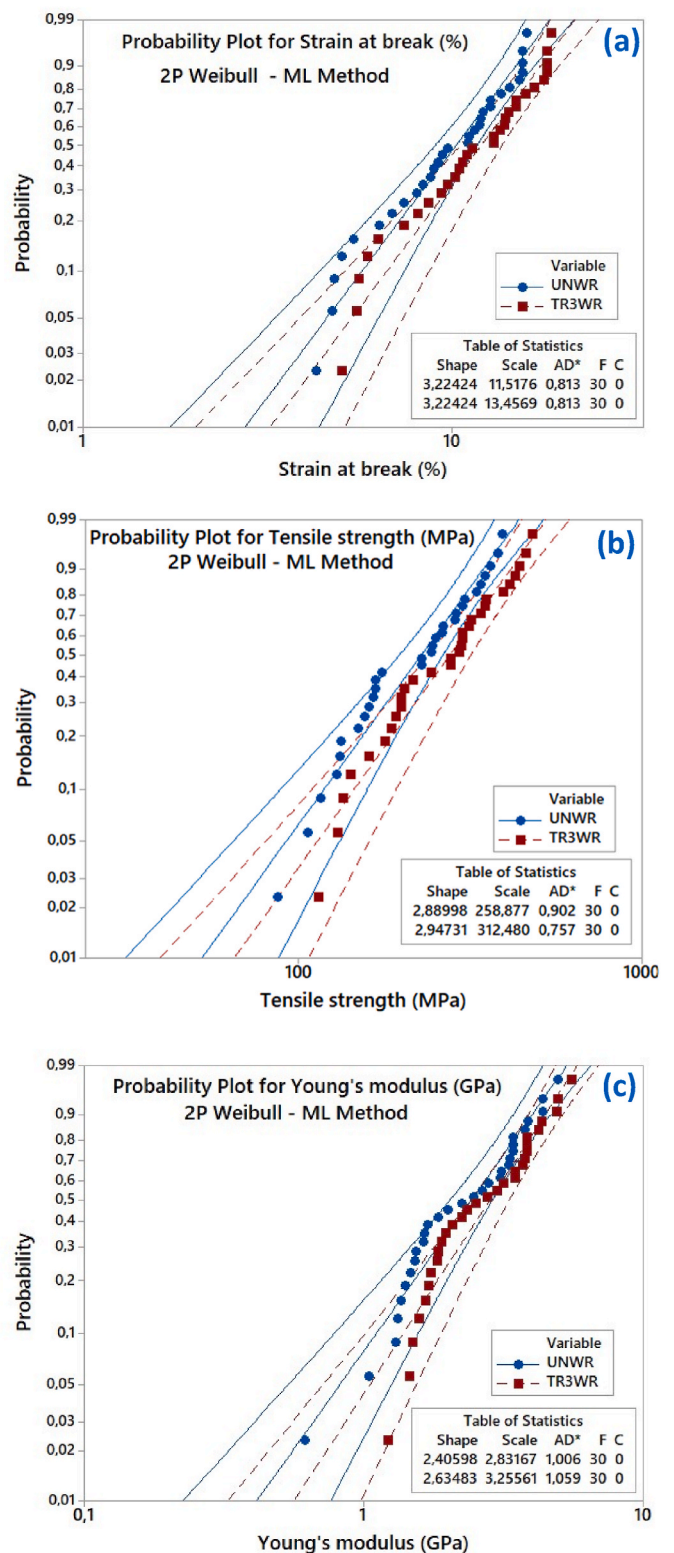


Fig. 3. Two-parameter Weibull distribution for mechanical properties by the ML method of untreated WR fibers and treated with 3% NaOH (a) tensile strain ( $\epsilon$ ), (b) tensile strength, and (c) Young's modulus.

### 3.2. Scanning electron microscopy (SEM) analysis

In the literature, SEM characterization has shown that vegetable fibers are covered with lignin [65], hemicellulose and pectin [66], and alkaline treatment of vegetable fibers eliminates impurities from their

**Table 3**Summary of the previously studied mechanical properties of different plant fibers (WR: *Washingtonia robusta*, WF: *Washingtonia filifera*, GL: Gauge length).

Material	Diameter ( $\mu\text{m}$ )	GL (mm)	Tensile strength (MPa)	Strain (%)	Young's modulus (GPa)	Ref.
Flax	18 $\pm$ 20	–	1036 $\pm$ 621	1.68 $\pm$ 0.95	54.52 $\pm$ 22.70	[101]
<i>Coccinia grandis</i> L.	27.33 $\pm$ 0.38	50	273 $\pm$ 27.74	2.703 $\pm$ 0.27	10.17 $\pm$ 1.26	[102]
<i>Juncus effusus</i> L.	280 $\pm$ 56	40	113 $\pm$ 36	2.75 $\pm$ 0.68	4.38 $\pm$ 1.37	[103]
<i>Agave sisalana</i>	240 $\pm$ 27	–	462 $\pm$ 71	7.83 $\pm$ 1.25	7.47 $\pm$ 1.37	[104]
<i>Lygeumspartum</i> L.	180 $\pm$ 433	40	280	1.49–3.74	13.2	[65]
<i>Furcraea foetida</i>	128	40	612.43 $\pm$ 52	10.45 $\pm$ 1.8	6.44 $\pm$ 2.1	[105]
<i>Hierochloe odorata</i>	136.7 $\pm$ 4.43	50	105 $\pm$ 35	2.37 $\pm$ 0.95	2.56 $\pm$ 0.98	[106]
<i>Dracaena draco</i>	–	–	553.13 $\pm$ 86.8	2.5 $\pm$ 0.42	24.9 $\pm$ 3.36	[107]
<i>Syagrus romanzoffina</i>	–	40	696	2.46	292	[21]
Flower agave	–	40	53.94	1.586	4.268	[108]
<i>Agave americana</i> L.	265 $\pm$ 80	40	142 $\pm$ 69	25.60 $\pm$ 8.25	2.14 $\pm$ 0.79	[109]
<i>Triplex halinus</i>	214 $\pm$ 531	40	64 $\pm$ 229	0.97 $\pm$ 2.61	6.60 $\pm$ 19.30	[110]
Untreated date palm	549 $\pm$ 027	50	125 $\pm$ 0.26	3.44 $\pm$ 0.23	4.52 $\pm$ 0.35	[111]
Date palm 2% NaOH (48 h)	333 $\pm$ 96	50	291.9 $\pm$ 0.28	4.10 $\pm$ 0.15	8.96 $\pm$ 0.35	[111]
WF	234 $\pm$ 43	40	119.3 $\pm$ 86.28	20.55 $\pm$ 11.08	2.34 $\pm$ 1.36	[63]
WF	227 $\pm$ 35	50	124.4 $\pm$ 80.08	23.21 $\pm$ 10.75	2.39 $\pm$ 1.26	[23]
WF	242 $\pm$ 39	10	204 $\pm$ 144	14.55 $\pm$ 9.11	3.03 $\pm$ 1.71	[64]
UNWR	330 $\pm$ 09	40	229 $\pm$ 89	10.28 $\pm$ 3.66	2.51 $\pm$ 1.4	This work
TR1WR	297 $\pm$ 24	40	233 $\pm$ 103	11.56 $\pm$ 3.82	2.59 $\pm$ 1.29	This work
TR2WR	288 $\pm$ 33	40	240 $\pm$ 78	11.98 $\pm$ 4.01	2.73 $\pm$ 1.63	This work
TR3WR	270 $\pm$ 008	40	243 $\pm$ 45	12.07 $\pm$ 4.28	2.88 $\pm$ 1.21	This work

surfaces [67]. This research investigated the consequences of alkaline treatment of WRFs with different concentrations of 1, 2 and 3% NaOH for 15 h of immersion at room temperature (RT). Fig. 5 illustrates the difference in surface area between untreated and alkaline-treated fibers. SEM obtained these morphological changes in raw and treated WRFs.

Before treatment (Fig. 5a), the fiber was covered with a lot of fat and impurities on the surface, which can be waxes, fats or amorphous substances such as pectin, lignin or hemicellulose; these substances make the surface of the fiber rigid. Some results in the literature are similar to ours, such as in work of Chilukoti et al. [68], who treated *Borassus palm* fibers with different concentrations of NaOH (2, 3, 4 and 5%) to determine the fibers' mechanical characteristics, morphology, and structure geometry. Fibers treated with 4% NaOH resulted in higher tensile strength, while a new alkali concentration level of 5% decreased tensile strength. Following the alkaline treatment of the fibers, the surface debris is eliminated; the higher the NaOH concentration, the smoother and less rigid the fiber surface becomes. This is due to the partial dissolution of the amorphous parts (pectin, lignin, and hemicellulose), which makes the diameter of the treated fibers smaller than that of the raw fibers. The observations on SEM images indicate the elimination of impurities with a weakening of the inner components of the fiber, such as hemicellulose and lignin, after the alkaline treatment, and this will be confirmed in the physical and thermal treatments of the fiber (FTIR, DSC, and TGA). (Fig. 5b–d).

The treatment of WRFs with NaOH and after drying increases the contact surface between the fibers and the interface. Except that it makes them associated and in the form of bunches, which requires the fibers to be ground to facilitate their adhesion to the matrix. SEM micrographic images of biocomposites tell us about the 'morphology' of the interfaces used, and it should be noted that a rough surface makes it possible to obtain a high number of anchoring points for the reinforcement fibers in the matrix and reduces stresses, which will form a good fiber-matrix bond [19]. Fig. 6 illustrates the different surface morphologies of micrographs of the four new biocomposites reinforced with raw and untreated short WR fibers and loaded with 1% biochar, which fills the structural gaps in the material, reduces surface defects, and facilitates load transfer between the PLA matrix and the reinforcing fibers. The surface morphology of the four biocomposites (Fig. 6a–d) continues to improve as the concentration of alkaline treatments of the fibers increases. Fig. 6d is that of the WRF-reinforced biocomposite treated with 3% NaOH, clearly showing the improvement in surface topology, which leads us to deduce that this is the most reinforced biocomposite of the others.

### 3.3. Fourier transform infrared (FTIR)

The FTIR spectroscopy helped us to identify the chemical reactions formed on the surfaces of the samples of the PLA/WR-BCH hybrid biocomposites produced. Fig. 7 shows the absorption spectra of untreated (UNWR) and treated (TR1WR, TR2WR and TR3WR) WRFs over a range of 4000 to 500  $\text{cm}^{-1}$ . The absorption point at 3352.33  $\text{cm}^{-1}$  indicates the extension vibrations of the free hydroxyl group (O–H) in the WRF, and this broadband associated with the cellulose (OH) bond decreases in intensity in the spectrum of fibers treated with 3% NaOH solution. The second band corresponds to the peak 2844.61  $\text{cm}^{-1}$ , the stretch of the aliphatic group (C–H) found in the spectra of the four samples, which gradually decreases following the removal of the hemicellulose [69]. The third band corresponds to phenomena of the elimination of non-cellulosic components such as pectin, lignin, and hemicellulose, with a decrease in the peak of 1726.05  $\text{cm}^{-1}$  in the sample of fibers not treated with NaOH, which is visible in the spectrum of the TR3WR sample. Lignin is present in the band at peak 1596.83  $\text{cm}^{-1}$  [70], followed by flexural stretching vibrations of the cellulose group at peak 1457.01  $\text{cm}^{-1}$ . The decrease continues to the peak of 1248.39  $\text{cm}^{-1}$  of the four samples, where the peak disappearance corresponds to the reduction of lignin on the surface of the NaOH-treated fibers due to stretching of the C=O bond of the acetyl group. The 1032.73  $\text{cm}^{-1}$  peak shows a decrease in the intensity of the cellulose bond, that of the hydroxyl group (OH), due to the fibers' alkaline treatment.

### 3.4. Thermogravimetric analysis (TGA)-Derivative thermogravimetry (DTG)

Untreated WRFs and fibers treated with different concentrations of NaOH were analyzed by TGA over a temperature range of 100–585  $^{\circ}\text{C}$ , to understand the impact of the alkaline treatment on the thermal stability of WRFs. Fig. 8 shows that there are two stages of fiber degradation, the first occurring between temperatures of 100 and 250  $^{\circ}\text{C}$ , which corresponds to the vaporization of water molecules (slight decrease) in these fibers. The second step of fiber degradation included from 250 to 400  $^{\circ}\text{C}$ , with untreated fibers starting with the deterioration of lignin and hemicellulose at 150  $^{\circ}\text{C}$  and finishing around 400  $^{\circ}\text{C}$  due to the drying and dehydration of the fibers, which is in accordance with the literature [71,72]. The decomposition of cellulose begins around 250  $^{\circ}\text{C}$  [73]. Furthermore, NaOH-treated fibers appear to have less thermal stability than untreated fibers. Fibers treated with 1% alkali show decomposition behavior identical to that of untreated fibers, while fibers

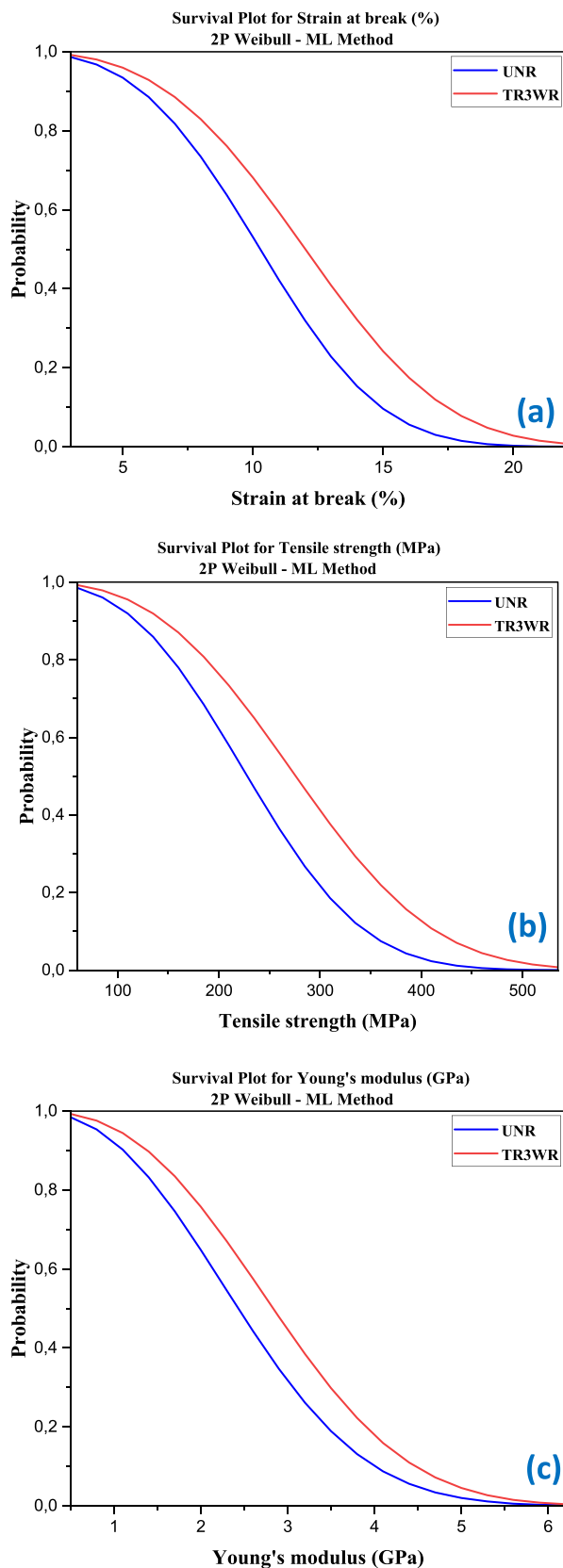


**Fig. 4.** Survival probability for 2P-Weibull-ML curves of mechanical properties for untreated WR fibers and treated with 3% NaOH (a) tensile strain ( $\epsilon$ ), (b) tensile strength, and (c) Young's modulus.

treated with 3% NaOH show less accelerated degradation compared with 2 and 1% treatment, despite the lower temperature.

Untreated and treated WRFs with different NaOH concentrations were thermally analyzed using TGA over a temperature range of 100–585 °C to understand the alkaline treatment's impact on the WRFs' thermal stability. Fig. 8 shows two fiber degradation stages, the first occurring between 100 and 250 °C, corresponding to the vaporization of water molecules (slight decrease) in these fibers. The second is included between 250 and 400 °C, with untreated fibers starting with the deterioration of lignin and hemicellulose at 150 °C and finishing around 400 °C due to the drying and dehydration of the fibers [71,72]. The cellulose decomposition begins around 250 °C [73]. Furthermore, NaOH-treated fibers appear to have less thermal stability than untreated fibers. Fibers treated with 1% alkali show decomposition behavior identical to untreated fibers, while fibers treated with 3% NaOH depict less accelerated degradation compared with 2 and 1% treatment, despite the lower temperature.

Table 4 shows the reduction in fiber weight occurring above 450 °C, equivalent to complete fibers' disintegration, defined by the phenomenon of carbon formation due to the thermal destruction of the fibers' cellulose components (hemicellulose, lignin, and cellulose). The most significant amount of carbon residue was found in the untreated fibers and those treated with 1% NaOH (27% for both samples). The fibers treated with 2% NaOH gave less carbon residue than the untreated and those treated with 1% NaOH (25%), and even better for those treated with 3% NaOH, which showed a minimum ash content of 22%. The four peaks in the derivative DTG curves (Fig. 9) correspond to the decomposition temperatures of the untreated fibers and fibers treated with 1, 2 and 3% NaOH.

A substantial decomposition is observed for all samples starting at 150 °C and continuing; this decomposition becomes complete above 410 °C [74,75]. The first peak of maximum degradation temperature of cellulosic structures is that of untreated UNR fibers at 321.123 °C, The second peak, that of TR1WR found at 322.4479 °C, the third peak that of TR2WR is less intense than the two previous ones and moves to a higher decomposition temperature value than all with a value of 340 °C; the decomposition starts at 158 °C and ends at 382 °C. The last peak, that of fibers treated with 3% NaOH, is less intense than the others, with a maximum decomposition at 326.537 °C, which means that there was an advanced decomposition of the fibers, starting at 165 °C and ending at 420 °C with carbon residues of 22 % of the primary mass. It should be emphasized that all these fibers underwent strong thermal and mechanical stresses during the alkaline treatment.

### 3.5. Differential scanning calorimetry (DSC)

Improving the composite's mechanical properties depends on the crystallinity percentage, which can increase if the cooling time is altered, as demonstrated in the study of PLA/cellulose nanocrystal nanocomposites by Doan et al. [73]. Fig. 10 shows the four peak melting temperatures ( $T_m$ ) for the four samples and the start and end temperatures for each fiber type. Table 5 shows the DSC results for untreated fibers and those treated with different concentrations of NaOH (1, 2 and 3%). The  $T_m$  of the four samples is defined from the significant peaks of the thermographs. The small peaks around the  $T_m$  of the different fibers and the curvature of the thermographs outside the melting range represent the impurities on the outer surface of the fibers that make them semi-crystalline [76,77]. The melting starting point defines  $T_m$ , and it can be seen that the peaks vary in shape and become narrower in order from the untreated UNWR fiber to TR1WR, then TR2WR to the TR3WR sample, which has the finest peak, meaning that it is the weakest in crystallization and therefore the most burnt; these fibers are organic and decompose quickly and melt in powder form. An examination of the  $T_m$  values illustrates that all of them are between 133 and 190 °C, with slight increases, the highest  $T_m$  being those of the fibers treated with 2% NaOH ( $T_m$  for TR2WR = 176 °C), while the  $T_m$  of the untreated fibers is

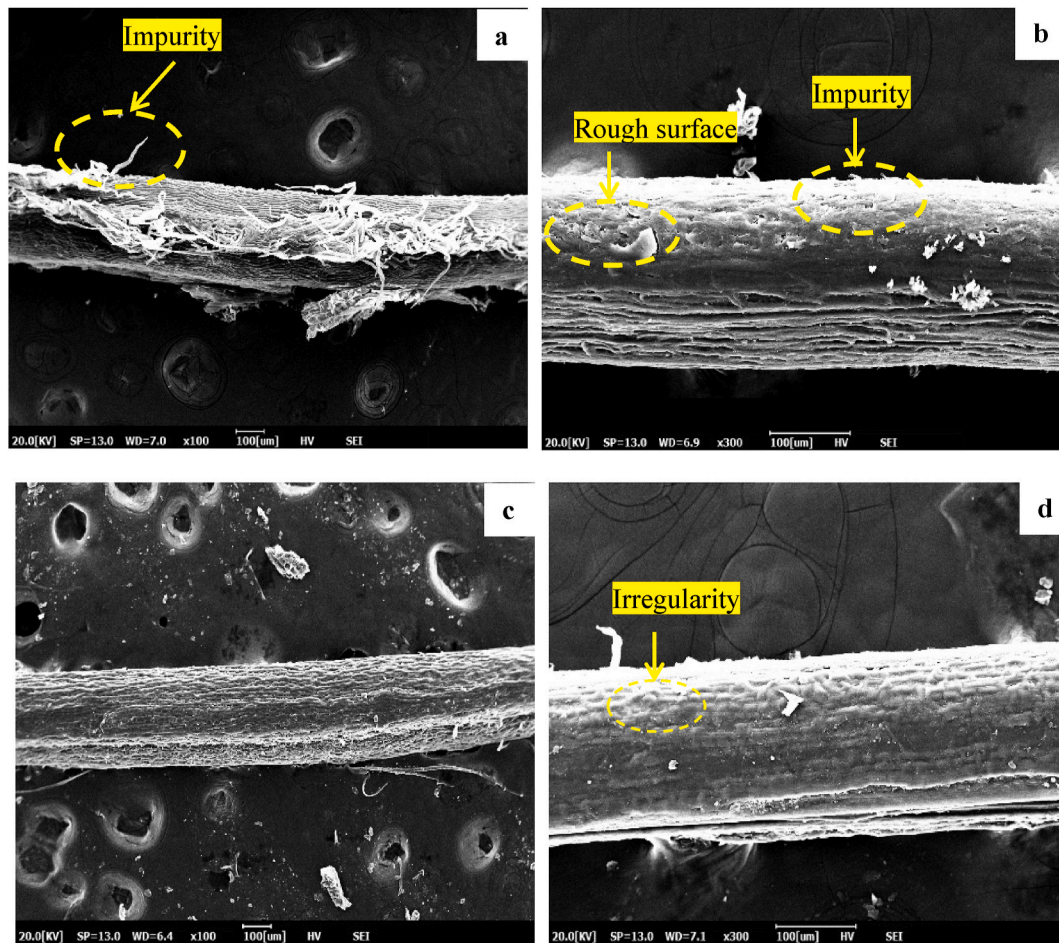


Fig. 5. Scanning electron microscope (SEM) images: (a) surface view of untreated WR fiber and (b–d) surface views of WRFs treated with 1, 2, and 3% of NaOH.

the lowest of the samples ( $T_m$  for UNWR = 158 °C), indicating a slight shift in the melting range of the samples. However, the slight increase in the  $T_m$  of the treated fibers compared with the  $T_m$  of the untreated fibers can be interpreted by the difference in the heat capacity of the fibers after treatment with different percentages of 1, 2 and 3 % alkaline solution. Crystallinity significantly influences the mechanical properties of composites [78], with an evolution of  $\sigma$ ,  $\epsilon$ , and E, as well as flexural strength.

### 3.6. Influence of the WR fibers' alkaline treatment on the mechanical behavior of the PLA/WR-BCH biocomposite

Tensile, flexural, and impact tests were conducted at RT to assess the mechanical specification of the developed hybrid biocomposites. Incorporating fibers treated with different NaOH concentrations into the PLA matrix improved the biocomposites' mechanical characteristics compared to untreated WR reinforcing fibers. Chaudhary et al. [79] have shown that hybridization of nettle-jute fibers in the jute/ortie/PLA biocomposite offers better mechanical behavior, such as tensile strength of 2.426 MPa, tensile modulus of 69.68 MPa, flexural strength of 157.33 MPa, flexural modulus of 16219.4 MPa and impact strength of 17.6 kg/cm<sup>2</sup> for jute/PLA, than the pure PLA biocomposite.

#### 3.6.1. Tensile test on PLA/WR-BCH biocomposite

To study the impact of WRFs' different alkaline surface treatments (1, 2 and 3% NaOH) on biocomposites' tensile strength and deformation with a PLA matrix filled with 1% BCH and reinforcing fibers, direct tensile tests have been conducted at RT on these biocomposites to compare them with the others developed. Fig. 11 shows the stress-strain

curves of samples UNB, BTR1, BTR2, and BTR3 (Table 2) in a tensile test using a Zwick machine with 5 kN capacity and 1 mm/min constant speed. Table 6 summarizes the tensile properties of the materials tested.

Note that all curves exhibit similar behavior and are divided into two phases; the first is very short and linear, known as the elastic phase, and the elastic stresses are 1.30, 1.71, 1.83 and 2.30 MPa for UNB, BTR1, BTR2, and BTR3, respectively. The maximum elastic stress is found for the BTR3, whereas the minimum value is observed for the untreated fiber-reinforced UNB. Then, in the second phase, the curve is quasi-linear, demonstrating that the maximum results of  $\sigma_t$  and  $\epsilon$  of this material are 31.11 MPa and 0.57%, respectively, for the UNB, and the material breaks just after the maximum tensile strength is reached, with E of 5.43 GPa.

Following the treatment of the reinforcement fibers, as depicted in Fig. 12, the tensile strength increases with the NaOH concentration. The maximum tensile strength values obtained for BTR3, BTR1, and BTR2 were 39.56, 32.73 and 36.12 MPa, respectively. These increases may be explained by the removal of impurities accumulated on the fibers' surface as a result of the alkaline treatment, reducing and dissolving lignin and hemicellulose on the fibers' surface [80], and facilitating their incorporation into the PLA matrix, which in turn improves the fiber-matrix interaction [66,81]. And this is consistent with the literature for other plant fibers treated with different soda concentrations and time durations for other matrices, such as Epoxy/WF [37], PLA/BF [82], unsaturated polyester/alfa [67], unsaturated polyester/date palm [83], polyester/sisal [84], polyester/coco [85].

Fig. 13 indicates that E decreases beyond the 2% WRF treatment concentration to 5.41 GPa (for the BTR3 material). In contrast, it increases progressively with the other biocomposites: 5.43, 5.6, and 5.8

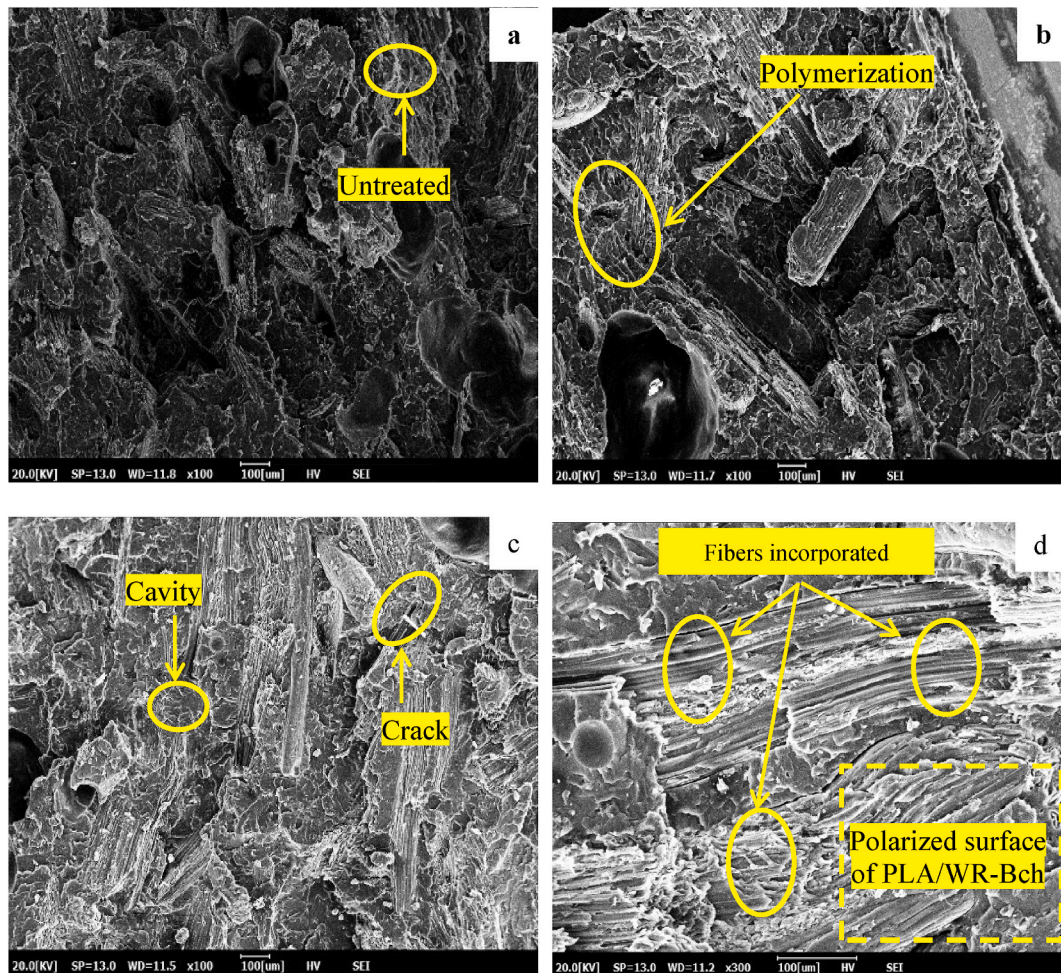


Fig. 6. Scanning electron microscope (SEM) images: (a) Surface view of the biocomposite reinforced with neutral WRFs and (b–d) Surface views of the biocomposites reinforced with WRFs treated with 1, 2, and 3% of NaOH.

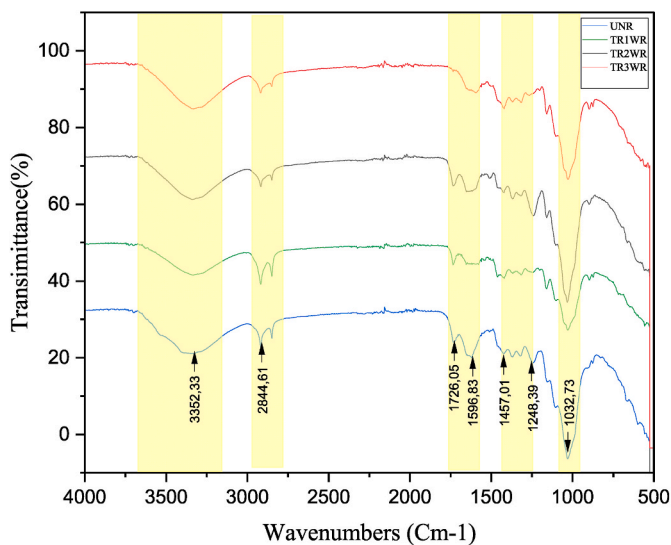


Fig. 7. Fourier transform infrared spectra of untreated and treated WRFs.

GPa for UNB, BTR1, and BTR2, respectively. It decreases either because of the high concentration of the NaOH solution or the duration of the treatment time (15 h), inducing an intense degradation of the internal structure of the fibers and thus influencing the mechanical

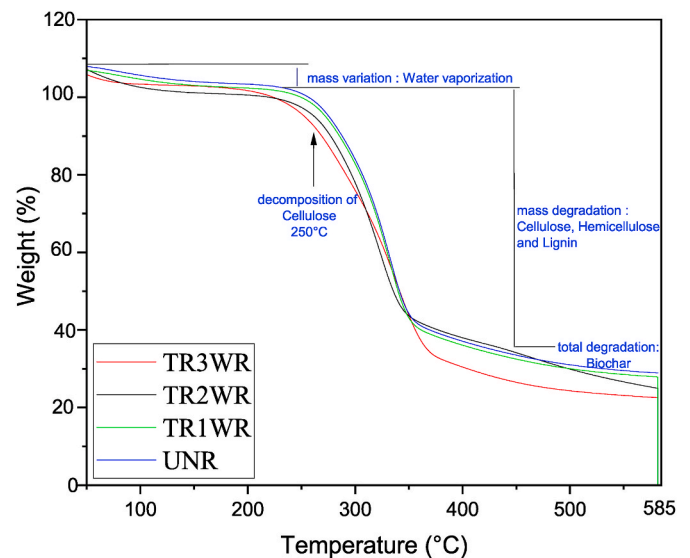
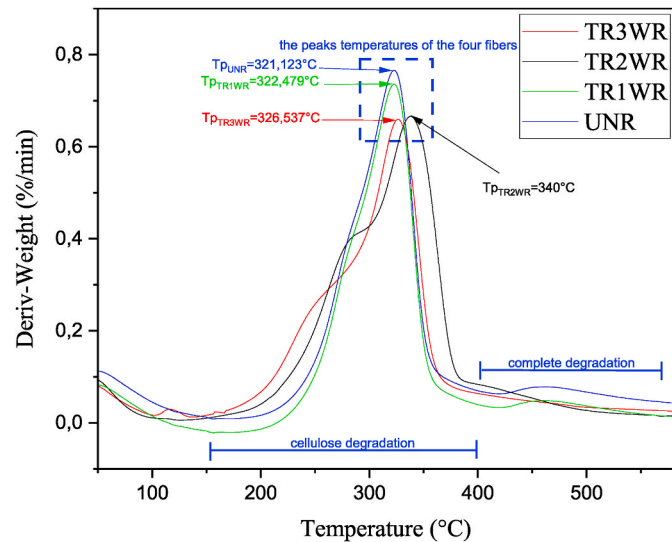


Fig. 8. Thermogravimetric analysis (TGA) curves of untreated and treated fibers at different concentrations of NaOH (1, 2 and 3%).

characteristics of the biocomposites. Fig. 14 shows the tensile strength and  $\sigma$  and E for untreated and treated WRF-reinforced composites, plotted on the same graph to illustrate the differences.

**Table 4**  
Thermogravimetric analysis (TGA) results of untreated and treated WR samples.

Fibers	First stage of degradation	Second stage of degradation	T (°C) at 60% of weight lost	T (°C) at 80% of weight lost	Remaining BCH (%) at 558 (°C)
UNR	100–214	234–359	326	303	27
TR1WR	100–214	232–359	326	303	27
TR2WR	100–215	229–379	320	296	25
TR3WR	100–232	207–420	324	289	22



**Fig. 9.** Derived weight-derivative thermogravimetry (DTG) as a function of temperature for neutral WR fibers and fibers treated with different concentrations of NaOH (1, 2 and 3%).

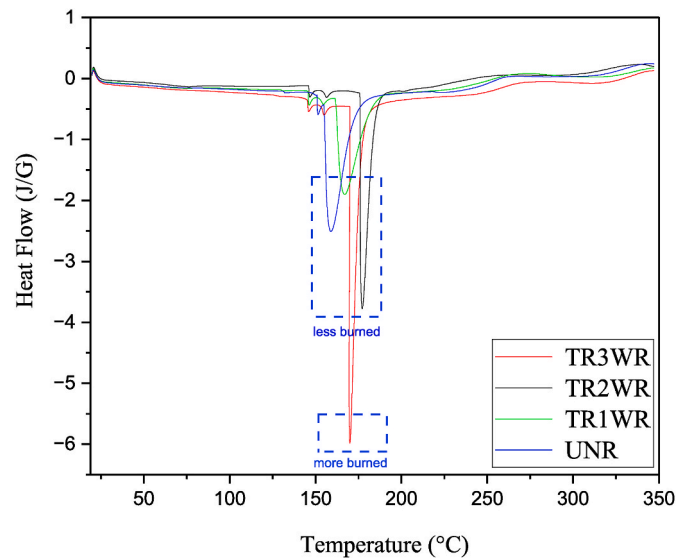


**Fig. 10.** Differential scanning calorimetry (DSC) curves for different neutral and NaOH treated fibers at different concentrations 1, 2, and 3% for the temperature of 25–350 °C and zoom of the selected area for a temperature of 140–200 °C.

**3.6.2. Flexural test on PLA/WR-BCH biocomposite**

As depicted in Fig. 15, the flexural strengths of the NaOH-treated WR-fiber composites are much higher than those of the untreated WR-fiber biocomposite (51.96 MPa). This is due to the void between the

**Table 5**  
Differential scanning calorimetry (DSC) results of untreated and treated WR samples.

Fibers	T start of melting (°C)	Melting temperature (°C)	T end of melting (°C)
UNR	133	158	189
TR1WR	133	168	189
TR2WR	140	176	193
TR3WR	141	170	190

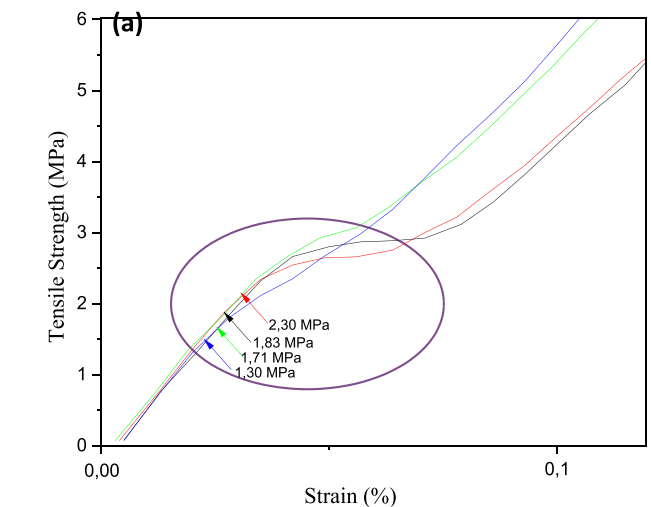
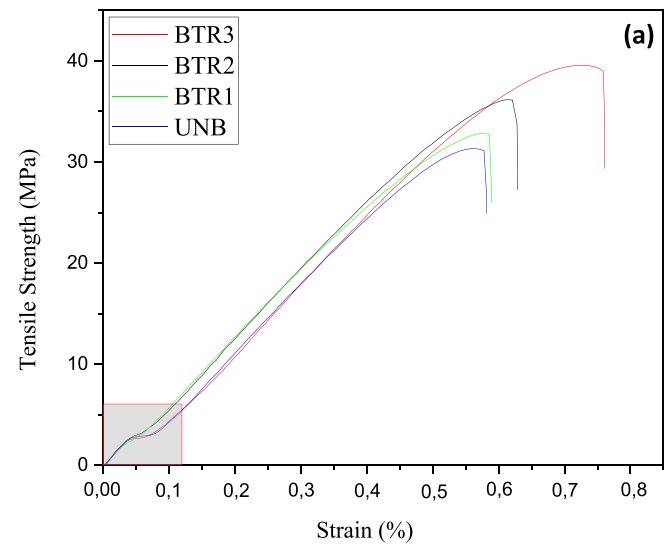


**Fig. 11.** Tensile stress-strain curve of PLA/WR-BCH biocomposites (UNB, BTR1, BTR2, BTR3) and zoom of the selected area for 0–0.1% strain.

fibers and the matrix; their adhesion improved with the increase in the percentage of alkaline treatment of the fibers. The BTR3 treated with 3% of NaOH shows the highest flexural strength (74.43 MPa) compared to the other two biocomposites, BTR2 (72.52 MPa) and BTR1 (62.74 MPa). So, we deduce that the strength of the fiber treated at 15 h in the NaOH solution increases and that 3% is the best since it coincides with the tensile strength results. The results of this study indicate that when the percentage of alkaline treatment is increased, the flexural strength of the reinforced biocomposite increases from that of the untreated fiber at 1% to that of the treated fiber at 2% to that of the treated fiber at 3%, as well as the flexural modulus (Table 6).

**Table 6**

Tensile and flexural mechanical properties of the biocomposites tested (WR: *Washingtonia robusta*, PLA: Polylactic acid, BCH: biochar).

Material	Mechanical properties				Reference
	Tensile strength (MPa)	Tensile modulus (GPa)	Flexural strength (MPa)	Flexural modulus (GPa)	
PLA/raw FEB	30.2	0.9	72.1	3.1	[82]
PLA/treated FEB	53.0	1.1	84.4	1.4	[82]
Polyester/Raw alfa	17.48	0.41	16.65	1.05	[67]
Polyester/alfa (T0724)	25.11	1.96	33.12	1.89	[67]
UP/10UDPF	26.72	0.58	65.88	2.68	[83]
UP/10TDPF	28.52	6.10	76.36	3.15	[83]
PLA/untreated WR-BCH	31.11	5.43	51.96	0.023	This work
PLA/1%treatedWR-BCH	32.73	5.6	62.74	0.026	This work
PLA/2%treatedWR-BCH	36.12	5.8	72.52	0.027	This work
PLA/3%treatedWR-BCH	39.56	5.41	74.43	0.027	This work

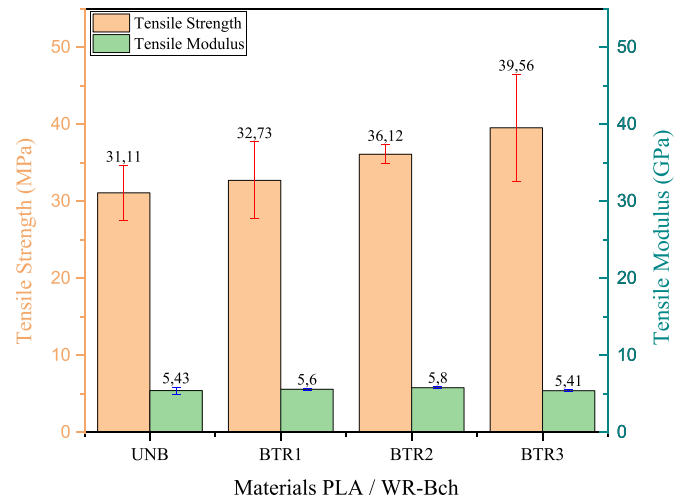
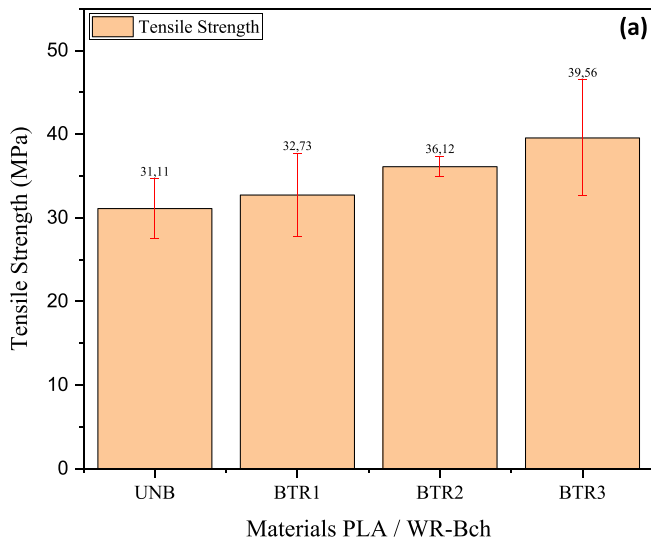


**Fig. 13.** Tensile strength-modulus histogram of PLA/WR-BCH biocomposites.

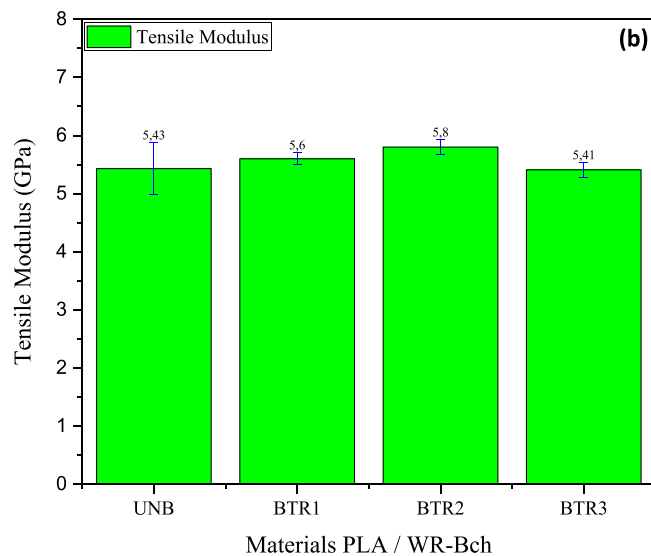


**Fig. 12.** Effect of alkaline treatment of WR Palm fiber on the tensile breaking stress and on the tensile modulus of biocomposites.

In addition, the third percentage gives a better flexural modulus (27.98 MPa) and an excellent fibers' surface treatment, which improves the biocomposite's mechanical characteristics and increases the fibers' adhesion to the PLA matrix, similar to the results reported in the literature for other reinforcement fibers.

Guo et al. [86] studied the mechanical properties by changing the

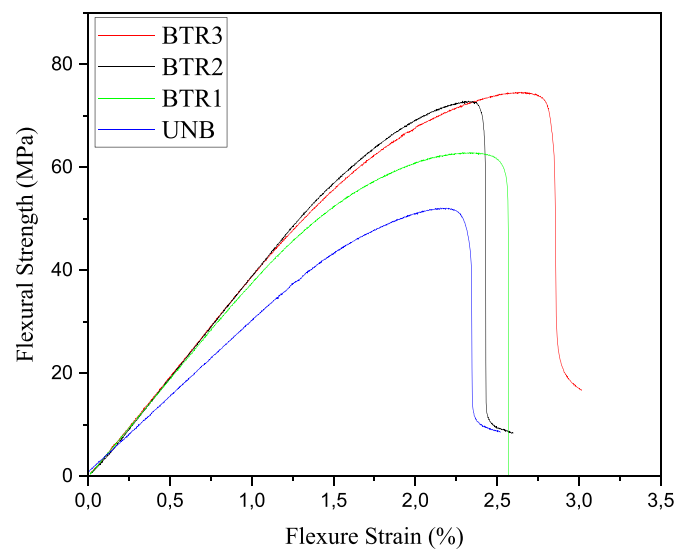


**Fig. 14.** Flexural strength-strain curves of PLA/WR-BCH biocomposites (UNB, BTR1, BTR2, and BTR3).

content of alkali-treated bamboo fibers (1, 3, 5 and 7%) and the cure time (1, 3 and 7 days). The composite had the best toughness when the alkali-treated bamboo fiber content was 3% by treatment [86]. Ochi [87] and Ouagne et al. [88] found that 6% alkaline treatment of kenaf fibers gave better results, whereas 9% destroyed the reinforcement fibers and caused them to adhere poorly to the PLA matrix. Several studies

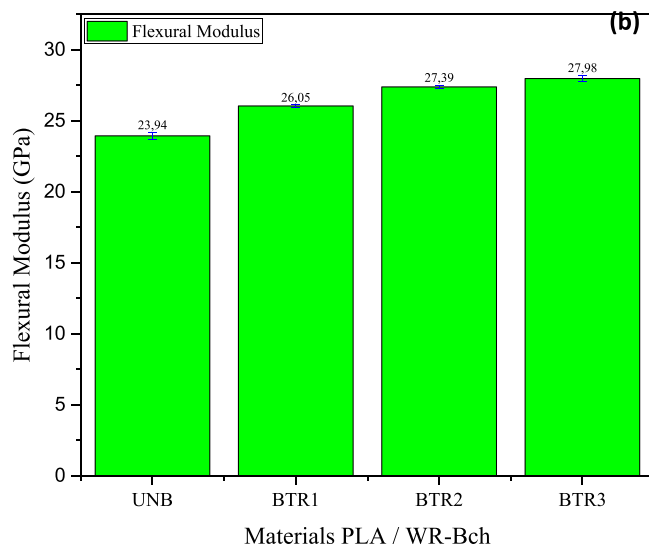
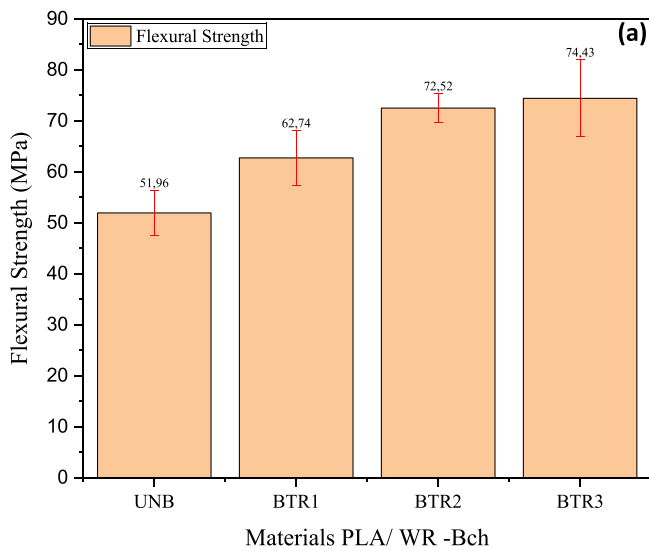


Fig. 15. Flexural strength and flexural modulus histogram of PLA/WR-BCH biocomposites.

have shown a relationship between the fibers’ distribution in their adhesion to the matrix and the biocomposite’s mechanical performance [89,83]. Accordingly, for a treatment of 15 h, the best NaOH concentration, i.e., the treatment that provides good protection for the fiber and improves the biocomposite’s mechanical behavior produced and high flexural-tensile strength, is 3%, despite the degradation of the tensile coefficient at this treatment level. Flexural strength and flexural modulus for untreated and treated WRF-reinforced composites are also plotted on histograms to illustrate the differences (Fig. 16).

### 3.6.3. Izod impact test of PLA/WR-BCH biocomposite

The primary purpose of an impact test is to determine a material’s impact absorption, resilience, and fracture toughness, as well as its resistance to impact and external load. Fig. 17 shows the difference in Izod impact resistance between the four biocomposites treated and untreated fiber reinforcement. The results are improving progressively from 1.785, 2.94, and 3.324 kJ/m<sup>2</sup> to its maximum value, which makes the BTR2 biocomposite the most absorbent of impact energy. The impact intensity decreases during the experiment with biocomposite BTR3 (3.262 kJ/m<sup>2</sup>), which contains a reinforcement of WR fibers treated with a 3% NaOH solution.

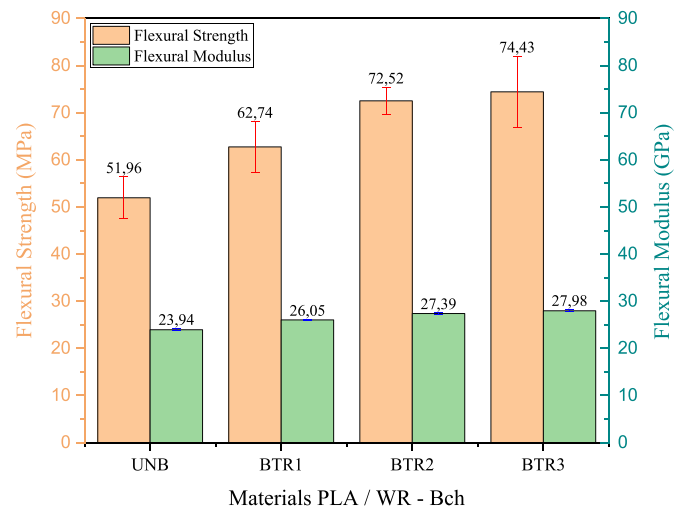


Fig. 16. Flexural strength and flexural modulus histogram of PLA/WR-BCH biocomposites.

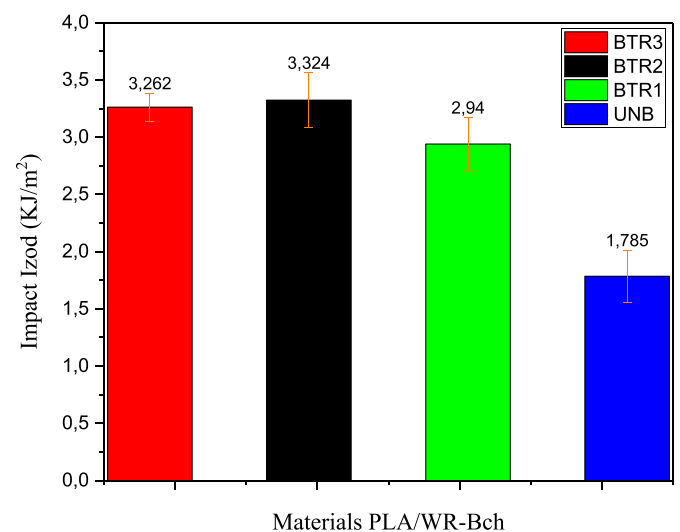


Fig. 17. Izod impact energy of the four PLA/WR-BCH biocomposites.

The increase in the impact resistance of biocomposites has been explained in other research [83] and is due to the strong adhesion of the fibers to the matrix [90,91] indeed, the reduction in the possibility of the material breaking, because these reinforcing fibers fill the voids and gaps in the matrix and make the material more resistant, thus requiring more energy to extract the fibers from the interface [92,93] and making the material less resistant to impact. The decrease in impact resistance for the BTR3 biocomposite indicates that the addition of these treated fibers, which are different from the previous ones and their incorporation into the PLA interface has led to a decrease in resilience, which can cause serious breakage of the material. The major cause of this reduction is the tearing of the internal structure of the fibers of the WR palm treated for 15 h with NaOH at a concentration of 3%, which makes them less adhesive to the PLA matrix, so the material absorbs less energy during impact. Many researchers in the literature have studied the impact of mass loading of WFFs in high-density polyethylene resin or polyethylene resin, reported by Lekrine et al. [64]. A decrease in impact resistance was observed in the work of Hristov et al. [94], which makes impact resistance very sensitive to the choice of reinforcement fibers treated for WR and the PLA matrix.

The increase in the impact resistance of biocomposites has been explained in other research [83]. It is due to the strong adhesion of the

fibers to the matrix [90,91] and the reduction in the possibility of the material breaking because these reinforcing fibers fill the voids and gaps in the matrix and make the material more resistant, thus requiring more energy to extract the fibers from the interface [92,93] and making the material less resistant to impact. The decrease in impact resistance for the BTR3 biocomposite indicates that the addition of these treated fibers, which are different from the previous ones and their incorporation into the PLA interface has led to a decrease in resilience, which can cause severe breakage of the material. The primary cause of this reduction is the tearing of the internal structure of the fibers of the WR palm treated for 15 h with NaOH at a concentration of 3%, which makes them less adhesive to the PLA matrix. Hence, the material absorbs less energy during impact. Many researchers have studied the effects of mass loading of WFFs in high-density polyethylene resin or polyethylene resin, as reported by Lekrine et al. [64]. A decrease in impact resistance was observed in the work of Hristov et al. [94], which shows the importance of the choice of WR reinforcement fiber treatments for the PLA matrix and their impact on the mechanical performance of the composite such as impact resistance.

### 3.6.4. Water absorption behavior

At different NaOH concentrations (0, 1, 2 and 3%), this section aimed to study the water absorption aspect of the PLA bioplastic interface and the PLA/WR-BCH biocomposites. The samples were immersed for 28 days in ambient air. The first observation is the amount of water that can be absorbed by the untreated fiber (0% NaOH), which can reach 250% of its initial mass before tube immersion in distilled water. This is due to its internal structure [95] and hydrophobicity [96]. As a result, the water saturation rate of raw fibers is much higher than that of the interface or the biocomposites produced. The matrix durability results show that PLA absorbs a shallow water level from a prolonged immersion time of over 408 h with a percentage of 0.5%; this behavior is almost the same as that of Deroiné et al. [97]. Fig. 18 also shows the development of the percentage water absorption of biocomposites, which is described in the literature by Fick's law [98–100]. This development translates into a difference in the saturation points of the biocomposites; it increases with the increase in the degree of alkaline treatment of the reinforcement fibers, is linear at first, and then changes and stabilizes in the saturation points: 5.126, 5.53, 7.55 and 8.31% of the UNB materials, BTR1, BTR2 and BTR3 respectively, which makes BTR3 the most water-absorbent since its cellulose and hemicellulose content is higher than that of the other biocomposites.

## 4. Summary and conclusions

This study highlights the positive impact of alkaline treatments applied to *Washingtonia robusta* (WR) palm fibers on the properties of biocomposites. This plant represents an innovation in the field of biocomposites. A thorough understanding of the interactions between the treatments, the fibers, and the Poly(lactic Acid) (PLA) interface paves the way for future research aimed at optimizing biocomposites based on natural resources. For the first time, a detailed analysis of the morphology, thermo-physicochemical, and mechanical properties of *Washingtonia robusta* fibers (WRFs) has been conducted, leading to the development of a new fully biodegradable hybrid biocomposite. The main conclusions to be drawn from this work are as follows:

Scanning Electron Microscope (SEM) revealed that the TR3WR fiber exhibited an improved surface that was smoother and less rough, with effective removal of impurities. Furthermore, the biocomposites examined under SEM showed that BTR3 displayed better adhesion between the fibers treated with 3% NaOH and the PLA interface.

Thermal treatments also demonstrated that the best thermal stability was achieved with the BTR3 biocomposite, illustrated by the removal of lignin and hemicellulose, as evidenced by Fourier Transform Infrared (FTIR) and Thermogravimetric Analysis (TGA) analyses. This material reached optimal thermal stability with a minimal ash content weight

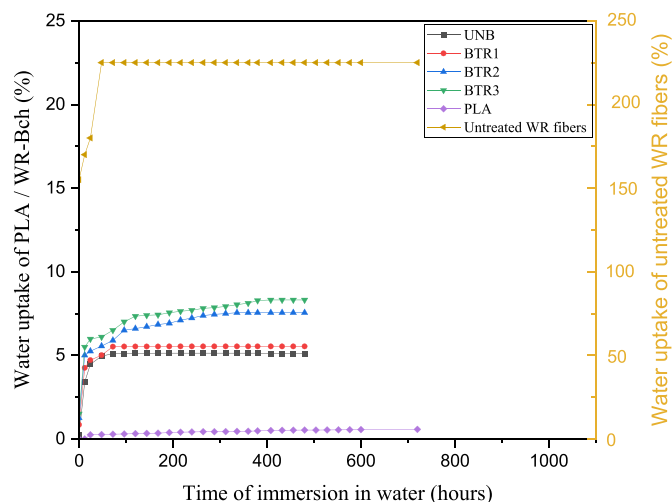


Fig. 18. Water absorption of untreated WR fibers, PLA matrix, and PLA/WR-BCH biocomposites.

loss of 22% at 450 °C, compared to the other biocomposites. Differential Scanning Calorimetry (DSC) corroborated our results, highlighting the greater crystallization of fibers treated with 3% NaOH, although all samples easily decomposed into a powder.

Moreover, the alkaline treatment of the WRF altered the surface of the reinforcing fibers and positively impacted the mechanical properties of the biocomposites compared to those made from untreated fibers. While the BTR3 exhibited maximum tensile and flexural strengths of 39.56 and 74.43 MPa, respectively, the tensile modulus decreased to 5.41 GPa after reaching a maximum value of 5.8 GPa for the BTR2 biocomposite. The flexural modulus results for biocomposites BTR2 and BTR3 were identical (27.98 GPa). The impact resistance peaked for the biocomposite reinforced with fibers treated with 2% NaOH after 15 h of immersion (3673 kJ/m<sup>2</sup>), surpassing the other biocomposites, including those with untreated fiber reinforcement and those treated with 1 and 3% NaOH. The BTR2 composite showed the best bonding between the WRF and the PLA matrix, and it was found that the optimal alkaline treatment was 2% NaOH after 15 h of immersion. Beyond this point, the fibers deteriorated, limiting their load-bearing capacity, which led to a decrease in the impact resistance of the composite with the 3% alkaline treatment.

Finally, the moisture uptake of the produced biocomposites increased with longer immersion times and higher concentrations of alkaline treatment applied to the reinforcing fibers, in comparison to both the PLA matrix and the untreated WR fibers.

In future work, we aim to capitalize on the time and mass of biochar to maximize the utilization of the tons of waste generated by WR each year the pruning of these decorative palms, which are prevalent both nationally and globally. By doing so, we hope enhance the profitability of WR palm applications.

## Funding

The authors acknowledge the financial support provided by research grant no. 12N233 from the United Arab Emirates University.

## Declaration of competing interest

The authors declare that they have no known competing financial interests or personal relationships that could have appeared to influence the work reported in this paper.

## References

- [1] Atikah MSN, et al. Degradation and physical properties of sugar palm starch/sugar palm nanofibrillated cellulose bionanocomposite. *Polimery* 2019;64(10):680–9. <https://doi.org/10.14314/polimery.2019.10.5>.
- [2] Ghernaout D, et al. Effects of incorporating cellulose fibers from *Yucca treculeana* L. on the thermal characteristics of green composites based on high-density polyethylene: an eco-friendly material for cleaner production. *J Mater Res Technol* 2024;31:787–98. <https://doi.org/10.1016/j.jmrt.2024.06.089>.
- [3] Allwood JM, Cullen JM, Milford RL. Options for achieving a 50% cut in industrial carbon emissions by 2050. *Environ Sci Technol Mar.* 2010;44(6):1888–94. <https://doi.org/10.1021/es902909k>.
- [4] Allwood JM, Ashby MF, Gutowski TG, Worrell E. Material efficiency: a white paper. *Resour Conserv Recycl* 2011;55(3):362–81. <https://doi.org/10.1016/j.resconrec.2010.11.002>.
- [5] Lin T, Jia D, Wang M, He P, Liang D. Effects of fibre content on mechanical properties and fracture behaviour of short carbon fibre reinforced geopolymer matrix composites. *Bull. Mater. Sci. Feb.* 2009;32:77–81. <https://doi.org/10.1007/s12034-009-0011-2>.
- [6] Assaedi H, Alomayri T, Shaikh F, Low I. Characterisation of mechanical and thermal properties in flax fabric reinforced geopolymer composites. *J. Advan. Ceram. Sep.* 2015;4:1–10. <https://doi.org/10.1007/s40145-015-0161-1>.
- [7] Ladaci N, et al. ANN and RSM prediction of water uptake of recycled HDPE biocomposite reinforced with treated palm waste W. Filifera. *J Nat Fibers Dec.* 2024;21(1):2356697. <https://doi.org/10.1080/15440478.2024.2356697>.
- [8] Mahdi E, Ochoa DRH, Vaziri A, Dean A, Kucukvar M. Khalasa date palm leaf fiber as a potential reinforcement for polymeric composite materials. *Compos Struct* 2021;265:113501. <https://doi.org/10.1016/j.compstruct.2020.113501>. Elsevier Ltd.
- [9] Plackett D, Løgstrup Andersen T, Batsberg Pedersen W, Nielsen L. Biodegradable composites based on l-poly lactide and jute fibres. *Compos Sci Technol* 2003;63(9):1287–96. [https://doi.org/10.1016/S0266-3538\(03\)00100-3](https://doi.org/10.1016/S0266-3538(03)00100-3). Elsevier Ltd., Oxford.
- [10] V Pastukhov L, Govaert LE. Crack-growth controlled failure of short fibre reinforced thermoplastics: influence of fibre orientation. *Int J Fatig* 2021;143:105982. <https://doi.org/10.1016/j.ijfatigue.2020.105982>. Elsevier Ltd.
- [11] W. Yun-ni et al., "The Variation of Biomass of Larix principis-rupprechtii Plantation along Slopes and Its Scale Effect in the Xiangshuihe Watershed of Liupan Mountains of China, Ningxia," *For Res*, vol. 28, no. 5, pp. 701–707, [Online]. Available: <http://www.lykxyj.com/article/id/20150515>.
- [12] Liu L, et al. Highly stretchable, sensitive and wide linear responsive fabric-based strain sensors with a self-segregated carbon nanotube (CNT)/Polydimethylsiloxane (PDMS) coating. *Prog Nat Sci: Mater Int* 2022;32(1):34–42. <https://doi.org/10.1016/j.pnsc.2021.10.012>.
- [13] Xiang D, et al. Synergistic effects of hybrid conductive nanofillers on the performance of 3D printed highly elastic strain sensors. *Compos Appl Sci Manuf* 2020;129:105730. <https://doi.org/10.1016/j.compositesa.2019.105730>.
- [14] Xiang D, et al. Enhanced performance of 3D printed highly elastic strain sensors of carbon nanotube/thermoplastic polyurethane nanocomposites via non-covalent interactions. *Compos B Eng* 2019;176:107250.
- [15] Xiang D, et al. 3D-Printed flexible piezoresistive sensors for stretching and out-of-plane forces. *Macromol Mater Eng Nov.* 2021;306(11):2100437. <https://doi.org/10.1002/mame.202100437>.
- [16] Masseteau B, Roy A, Michaud F, Irle M. Solutions composites bio-sourcées pour l'aviation légère : Modélisation du module d'élasticité en traction. *Jun.* 2011.
- [17] Bordoloi U, Kalita P. Experimental investigation on the stability of biocomposite phase change materials for building applications. 2024. p. 137–47. [https://doi.org/10.1007/978-3-031-48902-0\\_10](https://doi.org/10.1007/978-3-031-48902-0_10).
- [18] Workiyi A, Woldesenbet E. Development of maize stalk cellulose fiber reinforced calcined kaolinite clay geopolymer composite. *Proceed. Eng. Technol. Innovat.* 2020;16:30.
- [19] Workiyi A, Woldesenbet E. Flexural strength and porosity of NaOH-treated maize stalk cellulose-fibers-reinforced geopolymer composites. *Proceed. Eng. Technol. Innovat.* Aug. 2023;25:44–53. <https://doi.org/10.46604/peti.2023.10285>.
- [20] Belaadi A, et al. Extraction and characterization of a new lignocellulosic fiber from *Yucca treculeana* L. leaf as potential reinforcement for industrial biocomposites. *J Nat Fibers* 2022;19(15):12235–50.
- [21] Ferfari O, Belaadi A, Bedjaoui A, Alshahrani H, Khan MKA. Characterization of a new cellulose fiber extracted from *Syagrus Romanzoffiana* rachis as a potential reinforcement in biocomposites materials. *Mater Today Commun* 2023;36:106576. <https://doi.org/10.1016/j.jmtcomm.2023.106576>.
- [22] Lalaymia I, Belaadi A, Bedjaoui A, Alshahrani H, Khan MKA. Extraction and characterization of fiber from the flower stalk of the Agave plant for alternative reinforcing biocomposite materials. *Bio. Convers. Biorefine.* 2023. <https://doi.org/10.1007/s13399-023-04782-w>.
- [23] Dembri I, Belaadi A, Boumaaza M, Bourchak M. Tensile behavior and statistical analysis of *Washingtonia filifera* fibers as potential reinforcement for industrial polymer biocomposites. *J Nat Fibers May* 2022;1–16. <https://doi.org/10.1080/15440478.2022.2069189>.
- [24] Belaadi A, Boumaaza M, Alshahrani H, Bourchak M. Mechanical properties of natural cellulosic *Yucca treculeana* L. Fiber for biocomposites applications: statistical analysis. *J Nat Fibers Dec.* 2022;19(17):15501–18. <https://doi.org/10.1080/15440478.2022.2128505>.
- [25] Boumaaza M, Belaadi A, Bourchak M, Jawaid M, Satha H. Comparative study of flexural properties prediction of *Washingtonia filifera* rachis biochar bio-mortar by ANN and RSM models. *Construct Build Mater* 2022;318:125985. <https://doi.org/10.1016/j.conbuildmat.2021.125985>.
- [26] Poulouse AM, et al. Date palm biochar-polymer composites: an investigation of electrical, mechanical, thermal and rheological characteristics. *Sci Total Environ* 2018;619–620:311–8. <https://doi.org/10.1016/j.scitotenv.2017.11.076>.
- [27] Chai BX, Wang J, Dang TK, Nikzad M, Eisenbart B, Fox B. Comprehensive composite mould filling pattern dataset for process modelling and prediction. *J. Compos. Sci.* 2024;8(4). <https://doi.org/10.3390/jcs8040153>.
- [28] Chai B, et al. Review of approaches to minimise the cost of simulation-based optimisation for liquid composite moulding processes. *Materials Dec.* 2023;16:7580. <https://doi.org/10.3390/ma16247580>.
- [29] Zhang Q, Shi L, Nie J, Wang H, Yang D. Study on poly (lactic acid)/natural fibers composites. *J Appl Polym Sci* 2012;125(S2):E526–33.
- [30] Yen D, Phuong H, Chien N, Phuong D, Nguyen T. Study on plasticizing PLA using natural plasticizers available in Vietnam as a matrix resin for biodegradable PLA/cellulose composites. *Vietnam J. Chem. Mar.* 2024. <https://doi.org/10.1002/vjch.202300292>.
- [31] Wang W, et al. Development of bio-based PLA/cellulose antibacterial packaging and its application for the storage of shitake mushroom. *Food Chem Jul.* 2023;429:136905. <https://doi.org/10.1016/j.foodchem.2023.136905>.
- [32] Ozyhar T, Baradel F, Zoppe J. Effect of functional mineral additive on processability and material properties of wood-fiber reinforced poly (lactic acid) (PLA) composites. *Compos Appl Sci Manuf* 2020;132:105827.
- [33] Freitas PA, Gonzalez-Martinez C, Chiralt A. Stability and composting Behaviour of Pla-Starch Laminates containing Active extracts and cellulose fibres from rice Straw. 2024. <https://doi.org/10.20944/preprints202404.1161.v1>.
- [34] Sharma A, et al. Finite element modelling and analysis of jute fibre reinforced PLA matrix composite. *Mater Today Proc Apr.* 2024. <https://doi.org/10.1016/j.matpr.2024.04.056>.
- [35] Khelifi A, et al. Effects of alkaline treatment of *Washingtonia* mesh waste on the mechanical and physical properties of bio-mortar: experimental and prediction models. *Bio. Convers. Biorefine.* 2024;14(9):10621–50. <https://doi.org/10.1007/s13399-023-04221-w>.
- [36] Koadri Z, Benyahia A, Deghfel N, Belmokre K, Nouibat B, Redjem A. Étude de l'effet du temps de traitement alcalin de fibres palmier sur le comportement mécanique des matériaux à base d'argile rouge de la région de M'sila. *Matériaux Tech* 2019;107(4).
- [37] Dembri I, Belaadi A, Boumaaza M, Alshahrani H, Bourchak M. Drilling performance of short *Washingtonia filifera* fiber-reinforced epoxy biocomposites: RSM modeling. *Int J Adv Des Manuf Technol* 2022;121(11):7833–50. <https://doi.org/10.1007/s00170-022-09849-y>.
- [38] Islam M. The influence of Fibre processing and treatments on hemp Fibre/epoxy and hemp Fibre/PLA composites. *Jan.* 2009.
- [39] Anerao P, Kulkarni A, Munde Y, Shinde A, Das O. Biochar reinforced PLA composite for fused deposition modelling (FDM): a parametric study on mechanical performance. *Composites Part C: Open Access* 2023;12(September):100406. <https://doi.org/10.1016/j.jcomc.2023.100406>.
- [40] Huang C-C, Chang C-W, Jahan K, Wu T-M, Shih Y-F. Effects of the grapevine biochar on the properties of PLA composites. *Materials Jan.* 2023;16:816. <https://doi.org/10.3390/ma16020816>.
- [41] Jurczyk S, Andrzejewski J, Piasecki A, Musioł M, Rydz J, Kowalczyk M. Mechanical and rheological evaluation of polyester-based composites containing biochar. *Polymers Apr.* 2024;16:1231. <https://doi.org/10.3390/polym16091231>.
- [42] Zapata R, Palma Ramirez D, Pérez J, Rosales H, Díaz B, Adame A. Mechanical and thermal evaluation of PLA/PLA-g-MA/MCC composites via reactive extrusion. *MRS Advan.* 2023;8(Nov). <https://doi.org/10.1557/s43580-023-00683-2>.
- [43] Lekrine A, et al. Thermomechanical and structural analysis of green hybrid composites based on polylactic acid/biochar/treated W. Filifera palm fibers. *J Mater Res Technol* 2024. <https://doi.org/10.1016/j.jmrt.2024.06.033>.
- [44] Oka M. PLA and cellulose based degradable polymer composites. *Jan.* 2010.
- [45] Brunsek R, Dragana K, Schwarz I, Marasović P. Biodegradation properties of cellulose fibers and PLA biopolymer. *Polymers Aug.* 2023;15:3532. <https://doi.org/10.3390/polym15173532>.
- [46] Gao T, et al. Force model of ultrasonic empowered minimum quantity lubrication grinding CFRP. *Int J Mech Sci* 2024;280:109522. <https://doi.org/10.1016/j.ijmecsci.2024.109522>.
- [47] Liu D, et al. SiCp/Al composites from conventional to empowered machining: mechanisms and processability. *Compos Struct* 2024;346:118433. <https://doi.org/10.1016/j.compstruct.2024.118433>.
- [48] Gao T, et al. Mechanics analysis and predictive force models for the single-diamond grain grinding of carbon fiber reinforced polymers using CNT nanolubricant. *J Mater Process Technol* 2021;290:116976. <https://doi.org/10.1016/j.jmatprotec.2020.116976>.
- [49] Auras R, Harte B, Selke S. An overview of poly(lactides) as packaging materials. 2004. p. 835–64. <https://doi.org/10.1002/mabi.200400043>.
- [50] Jamshidian M, Tehrani EA, Imran M, Jacquot M. "Poly-Lactic acid : production. *Appl. Nano. Release Stud.* 2010;9:552–71. <https://doi.org/10.1111/j.1541-4337.2010.00126.x>.
- [51] Nampoothiri KM, Nair NR, John RP. Bioresource Technology an overview of the recent developments in polylactide (PLA) research. *Bioresour Technol* 2010;101(22):8493–501. <https://doi.org/10.1016/j.biortech.2010.05.092>.
- [52] Mehta R, Kumar V, Bhunia H, Upadhyay SN. "Synthesis of poly (lactic acid): a review synthesis of poly (lactic acid). *Review* 2006;1797. <https://doi.org/10.1080/15321790500304148>.

- [53] Astm E. 08: standard test method for oxidation onset temperature of hydrocarbons by differential scanning calorimetry. Annu Book ASTM (Am Soc Test Mater) Stand 2009.
- [54] A. International. ASTM D638-14, standard test method for tensile properties of plastics. ASTM International; 2015.
- [55] A. S. D. 10 on M. Properties. Standard test methods for flexural properties of unreinforced and reinforced plastics and electrical insulating materials. 1997.
- [56] Standard A. Standard terminology for additive manufacturing technologies, F2792–12a. ASTM International; 2012. p. 1–9.
- [57] Galgani F, Souplet A, Cadiou Y. Accumulation of debris on the deep floor off the French Mediterranean coast. *Mar. Ecol-Progr. Ser. Oct.* 1996;142:225–34. <https://doi.org/10.3354/meps142225>.
- [58] Ducros F, Pamphile P. Bayesian estimation of Weibull mixture in heavily censored data setting. *Reliab Eng Syst Saf* 2018;180:453–62. <https://doi.org/10.1016/j.res.2018.08.008>.
- [59] Rao KMM, Rao KM. Extraction and tensile properties of natural fibers: vakka, date and bamboo. *Compos Struct* 2007;77(3):288–95.
- [60] Tokoro R, Vu DM, Okubo K, Tanaka T, Fujii T, Fujiura T. How to improve mechanical properties of poly(lactic acid) with bamboo fibers. *J Mater Sci* 2008;43(2):775–87. <https://doi.org/10.1007/s10853-007-1994-y>.
- [61] Abderrezak B, Amroune S, Scarpa F. Statistical analysis and effect of chemical treatment on the physico-mechanical behavior of fibres from date-palm fruit branches. *Rev. Sci. Technol., Synthèse Jan.* 2015;31:108–20.
- [62] Amroune S, Bezazi A, Dufresne A, Scarpa F, Imad A. Investigation of the date palm fiber for green composites reinforcement: thermo-physical and mechanical properties of the fiber. *J Nat Fibers* 2019. <https://doi.org/10.1080/15440478.2019.1645791>.
- [63] Benzannache N, Belaadi A, Boumaaza M, Bourchak M. Improving the mechanical performance of biocomposite plaster/Washingtonian filifira fibres using the RSM method. *J Build Eng* 2021;33:101840. <https://doi.org/10.1016/j.job.2020.101840>.
- [64] Lekrine A, et al. Structural, thermal, mechanical and physical properties of Washingtonia filifera fibres reinforced thermoplastic biocomposites. *Mater Today Commun Jun.* 2022;31:103574. <https://doi.org/10.1016/j.mtcomm.2022.103574>.
- [65] Belouadah Z, Ati A, Rokbi M. Characterization of new natural cellulosic fiber from Lygeum spartum L. *Carbohydr Polym* 2015;134:429–37. <https://doi.org/10.1016/j.carbpol.2015.08.024>.
- [66] Mansour R, Osmani H, Imad A, Benseddiq N. Effect of chemical treatment on flexure properties of natural fiber-reinforced polyester composite. *Procedia Eng Dec.* 2011;10:2092–7. <https://doi.org/10.1016/j.proeng.2011.04.346>.
- [67] Melouki A, et al. Effect of alkaline treatment on mechanical properties of alfa fiber/unsaturated polyester composite. *Cellul Chem Technol Jul.* 2023;57:607–15. <https://doi.org/10.35812/CelluloseChemTechnol.2023.57.55>.
- [68] Chilukoti GR, Bairabathina V, Munagala S, Kumar K, C P, Periyasamy AP. Study of alkali treatment and its influence on characteristics of Borassus palm fiber. *J Nat Fibers May* 2022;19:1–12. <https://doi.org/10.1080/15440478.2022.2069197>.
- [69] Sreekala MS, Thomas S. Effect of fibre surface modification on water-sorption characteristics of oil palm fibres. *Compos Sci Technol* 2003;63(6):861–9.
- [70] Bessadok A, et al. Effect of chemical treatments of Alfa (*Stipa tenacissima*) fibres on water-sorption properties. *Compos Sci Technol* 2007;67(3–4):685–97.
- [71] Kim H-S, Yang H-S, Kim H-J, Park H-J. Thermogravimetric analysis of rice husk flour filled thermoplastic polymer composites. *J Therm Anal Calorim* 2004;76(2):395–404.
- [72] Kim H-S, Kim S, Kim H-J, Yang H-S. Thermal properties of bio-flour-filled polyolefin composites with different compatibilizing agent type and content. *Thermochim Acta* 2006;451(1–2):181–8.
- [73] Doan TTL. Investigation on jute fibres and their composites based on polypropylene and epoxy matrices. 2006.
- [74] Lemita N. Élaboration et Caractérisation de Structure Composite à Base de Matrice Organique Renforcée par de Nouvelles Fibres Cellulosiques Naturelles Extraites de la Plante *Strelitzia Reginae*. Université Echahid Cheikh Larbi-Tebessi-Tébessa 2023.
- [75] Rachini A, Peyratout C, Pagnoux C, Smith A. Cohésion à l'interface matrice minérale/fibres cellulosiques: traitements chimiques des fibres et caractérisation. *Matériaux Tech* 2012;100(5):401–11.
- [76] Berlioz S, Stinga C, Condoret J, Samain D. Sfgp 2007 - investigation of a novel principle of chemical grafting for modification of cellulose fibers 2008;6(1). <https://doi.org/10.2202/1542-6580.1672>.
- [77] Menczel JD, Kohl WS. "3 - differential scanning calorimetry (DSC) in fiber research,". In: Jaffe M, B JD, T T, of T A, Menczel F, editors. *The Textile Institute Book series*. Woodhead Publishing; 2020. p. 17–69. <https://doi.org/10.1016/B978-0-08-100572-9.00003-3>.
- [78] Sun H, et al. Electrical, mechanical and damage self-sensing properties of basalt fiber reinforced polymer composites modified by electrophoretic deposition. *Prog Nat Sci: Mater Int* 2023;33(5):593–600. <https://doi.org/10.1016/j.pnsc.2023.11.003>.
- [79] Chaudhary V, Radhakrishnan S, Das PP, Dwivedi S, Mishra S, Gupta P. Development and mechanical characterization of PLA composites reinforced with jute and nettle bio fibers. *Bio. Convers. Biorefine. Dec.* 2023. <https://doi.org/10.1007/s13399-023-05183-9>.
- [80] Yan L, Chouh N, Yuan X. Improving the mechanical properties of natural fiber fabric reinforced epoxy composites by alkali treatment. *J Reinforc Plast Compos Feb.* 2012;31(6):425–37. <https://doi.org/10.1177/0731684412439494>.
- [81] Ibrahim N, Hadithon K, Abdan K. Effect of fiber treatment on mechanical properties of kenaf fiber-ecoflex composites. *J. Reinf. Plast. Composite Jul.* 2010; 29:2192–8. <https://doi.org/10.1177/0731684409347592>.
- [82] Shih Y-F, Huang C-C. Poly(lactic acid (PLA)/banana fiber (BF) biodegradable green composites. *J Polym Res* 2011;18(6):2335–40. <https://doi.org/10.1007/s10965-011-9646-y>.
- [83] Samira M, Meftah Y, Bouchamia I, Benyaghla A. Alkali-treated date palm fiber-reinforced unsaturated polyester composites: thermo-mechanical performances and structural applications. *Iran Polym J (Engl Ed)* 2023;32(Sep). <https://doi.org/10.1007/s13726-023-01224-2>.
- [84] Sahai R, Biswas D, Yadav M, Samui A, Kamble S. Effect of alkali and silane treatment on water absorption and mechanical properties of sisal fiber reinforced polyester composites. *J Inst Eng Dec.* 2022;28:641–56. <https://doi.org/10.56801/MME864>.
- [85] Bakri B, Chandrabakty S. Influence of Alkali And Microwave Treatments of Fiber on The Water Absorption And The Mechanical Properties of Coir Fiber/Polyester Composites. 2018. <https://doi.org/10.2991/icmeme-18.2019.8>.
- [86] Guo C, Li M, Wang S, Zhang S, Li Y, Li C. Alkali treatment of bamboo fibers improves the mechanical properties of metakaolin geopolymer. *J Dispersion Sci Technol Mar.* 2023;45:1–10. <https://doi.org/10.1080/01932691.2023.2190391>.
- [87] Ochi S. Mechanical properties of kenaf fibers and kenaf/PLA composites. *Mech Mater* 2008;40(4):446–52. <https://doi.org/10.1016/j.mechmat.2007.11.4698>.
- [88] Ouagne P, et al. 5 - use of bast fibres including flax fibres for high challenge technical textile applications. Extraction, preparation and requirements for the manufacturing of composite reinforcement fabrics and for geotextiles. In: Kozłowski RM, of MBTH, Mackiewicz-Talarczyk NFE, editors. *The Textile Institute Book series*. Woodhead Publishing; 2020. p. 169–204. <https://doi.org/10.1016/B978-0-12-818782-1.00005-5>.
- [89] Zaghoul M, Zaghoul MM, Zaghoul M. Developments in polyester composite materials – an in-depth review on natural fibers and nano fillers. *Compos Struct Sep.* 2021;278:114698. <https://doi.org/10.1016/j.compstruct.2021.114698>.
- [90] Karaduman Y, Seçinti Klop H, Sahbaz Karaduman N. Ultrasonication-assisted alkali treatment of hemp fibers to improve the fiber/matrix interface of hemp/epoxy composites: the influence of sodium dodecyl sulfate surfactant. *Polym Compos Mar.* 2024. <https://doi.org/10.1002/pc.28333>.
- [91] Boominathan SK, Amutha V, Sentharamaikkannan P, Raj DVK, Selvaraj SK, Sakthivel S. Investigation of mechanical, thermal, and moisture diffusion behavior of Acacia concinna FIBER/POLYESTER matrix composite. *J Nat Fibers Nov.* 2022;19(16):13495–510. <https://doi.org/10.1080/15440478.2022.2099502>.
- [92] Baley C, Gominia M, Breard J, Bourmaud A, Davies P. Variability of mechanical properties of flax fibres for composite reinforcement . A review. 2019.
- [93] Kirgiz FPD. A critical Review on the properties of natural fiber and bio-resin: effect of alkali treatment. *Jul.* 2023.
- [94] Hristov V, Vasileva ST, Krumova M, Lach R, em G Prof, Michler Dr habil. Deformation mechanisms and mechanical properties of modified polypropylene/wood fiber composites. *Polym Compos Oct.* 2004;25:521–6. <https://doi.org/10.1002/pc.20045>.
- [95] Murugesan B, Chandrashekar J, Selvan S. Experimental investigation of natural fiber reinforced Concrete in Construction industry. *Jan.* 2022.
- [96] Jamshaid H, Ali H, Mishra R, Nazari S, Chandan V. Durability and accelerated ageing of natural fibers in concrete as a sustainable construction material. *Materials Oct.* 2023;16:6905. <https://doi.org/10.3390/ma16216905>.
- [97] Deroine M, et al. Accelerated ageing of polylactide in aqueous environments: comparative study between distilled water and seawater. *Polym Degrad Stab* 2014;108(Oct). <https://doi.org/10.1016/j.polydegradstab.2014.01.020>.
- [98] Saaidia A, Belaadi A, Boumaaza M, Alshahrani H, Bourchak M. Effect of water absorption on the behavior of jute and sisal fiber biocomposites at different lengths: ANN and RSM modeling. *J Nat Fibers Nov.* 2022;20:1–19. <https://doi.org/10.1080/15440478.2022.2140326>.
- [99] Makhoulouf A, Belaadi A, Boumaaza M, Mansouri L, Bourchak M, Jawaid M. Water absorption behavior of jute fibers reinforced HDPE biocomposites: prediction using RSM and ANN modeling. *J Nat Fibers Sep.* 2022;19:1–18. <https://doi.org/10.1080/15440478.2022.2114976>.
- [100] Mahdi E, Hernández Ochoa DR, Vaziri A, Dean A, Kucukvar M. Khalasa date palm leaf fiber as a potential reinforcement for polymeric composite materials. *Compos Struct* 2020. <https://doi.org/10.1016/j.compstruct.2020.113501>.
- [101] Belaadi A, Amroune S, Bourchak M. Effect of eco-friendly chemical sodium bicarbonate treatment on the mechanical properties of flax fibres: Weibull statistics. *Int J Adv Manuf Technol* 2020;106(5–6):1753–74. <https://doi.org/10.1007/s00170-019-04628-8>.
- [102] Sentharamaikkannan P, Kathiresan M. Characterization of raw and alkali treated new natural cellulosic fiber from *Coccinia grandis*.L. *Carbohydr Polym* 2018;186:332–43. <https://doi.org/10.1016/j.carbpol.2018.01.072>.
- [103] Maache M, Bezazi A, Amroune S, Scarpa F, Dufresne A. Characterization of a novel natural cellulosic fiber from *Juncus effusus*. *Carbohydr Polym* 2017;171:163–72. <https://doi.org/10.1016/j.carbpol.2017.04.096>.
- [104] Belaadi A, Bezazi A, Bourchak M, Scarpa F. Tensile static and fatigue behaviour of sisal fibres. *Mater Des* 2013;46:76–83. <https://doi.org/10.1016/j.matdes.2012.09.048>.
- [105] Manimaran P, Sentharamaikkannan P, Sanjay MR, Marichelvam MK, Jawaid M. Study on characterization of *Furcraea foetida* new natural fiber as composite reinforcement for lightweight applications. *Carbohydr Polym* 2018;181:650–8. <https://doi.org/10.1016/j.carbpol.2017.11.099>.

- [106] Dalmis R, Köktaş S, Seki Y, Kılınç AÇ. Characterization of a new natural cellulose based fiber from Hierochloe Odarata. *Cellulose* 2020;27(1):127–39. <https://doi.org/10.1007/s10570-019-02779-1>.
- [107] Hadou A, Belaadi A, Alshahrani H, Khan MKA. Extraction and characterization of novel cellulose fibers from Dracaena draco plant. *Mater Chem Phys* 2024;313: 128790. <https://doi.org/10.1016/j.matchemphys.2023.128790>.
- [108] Lalaymia I, Belaadi A, Boumaaza M, Alshahrani H, Khan MKA, Dib A. Weibull statistic and artificial neural network analysis of the mechanical performances of fibers from the flower Agave plant for eco-friendly green composites. *J Nat Fibers* Dec. 2024;21(1):2305228. <https://doi.org/10.1080/15440478.2024.2305228>.
- [109] Bezazi A, Belaadi A, Bourchak M, Scarpa F, Boba K. Novel extraction techniques, chemical and mechanical characterisation of Agave americana L. natural fibres. *Compos B Eng* 2014;66:194–203. <https://doi.org/10.1016/j.compositesb.2014.05.014>.
- [110] Belouadah Z, Toubal L, Belhaneche-Bensemra N, Ati A. Characterization of ligno-cellulosic fiber extracted from Atriplex halimus L. plant. *Int J Biol Macromol* 2020. <https://doi.org/10.1016/j.ijbiomac.2020.11.142>.
- [111] Amroune S, et al. Tensile mechanical properties and surface chemical sensitivity of technical fibres from date palm fruit branches (Phoenix dactylifera L.). *Compos Appl Sci Manuf* 2015;71. <https://doi.org/10.1016/j.compositesa.2014.12.011>.